NAVAL POSTGRADUATE SCHOOL

MONTEREY, CALIFORNIA

THESIS

ASYMMETRIC INFLUENCE OF SINGLE PROPELLER UUV OPERATIONS ON ENTANGLEMENT WITH MARINE VEGETATION

by

James M. Dubyoski

June 2022

Thesis Advisor: Joseph T. Klamo
Co-Advisor: Anthony G. Pollman

THIS PAGE INTENTIONALLY LEFT BLANK

REPORT DOCUMENTATION PAGE			*Form Approved OMB No. 0704-0188*

1. AGENCY USE ONLY *(Leave blank)*	**2. REPORT DATE** June 2022	**3. REPORT TYPE AND DATES COVERED** Master's thesis

4. TITLE AND SUBTITLE
ASYMMETRIC INFLUENCE OF SINGLE PROPELLER UUV OPERATIONS ON ENTANGLEMENT WITH MARINE VEGETATION

5. FUNDING NUMBERS

6. AUTHOR(S) James M. Dubyoski

7. PERFORMING ORGANIZATION NAME(S) AND ADDRESS(ES)
Naval Postgraduate School
Monterey, CA 93943-5000

8. PERFORMING ORGANIZATION REPORT NUMBER

9. SPONSORING / MONITORING AGENCY NAME(S) AND ADDRESS(ES)
N/A

10. SPONSORING / MONITORING AGENCY REPORT NUMBER

11. SUPPLEMENTARY NOTES The views expressed in this thesis are those of the author and do not reflect the official policy or position of the Department of Defense or the U.S. Government.

12a. DISTRIBUTION / AVAILABILITY STATEMENT
Approved for public release. Distribution is unlimited.

12b. DISTRIBUTION CODE
A

13. ABSTRACT (maximum 200 words)

This thesis continues previous work conducted on the interactions between a single propeller unmanned underwater vehicle (UUV) and marine vegetation. It attempts to define the asymmetric behavior of entanglement between a single, shroud-less propeller and synthetic eelgrass. A Disposable Reusable Expeditionary Warfare Underwater Vehicle (DREW UV), designed as a low-cost testing vehicle, was fixed at various test conditions in a towing tank. A four-factor full factorial design of experiments that varied lateral separation, depth, vehicle speed, and whether the eelgrass was on the port or starboard side of the vehicle was used to evaluate how these factors changed the likelihood of entanglement with a single strand of eelgrass. Each factor's impact was assessed as it pertained to which side of the vehicle the eelgrass was on. The tests revealed that significant asymmetry exists in the behavior of entanglement for a single propeller UUV based on the side of passage. The likelihood of entanglement is further reduced or increased based on the other variable factors. Thus, the asymmetry that exists does so on a scale. Certain test conditions can exacerbate this asymmetry and should be given consideration when applied to operational usage. Future work includes further testing to increase fidelity in results, testing to understand the stochastic nature of occlusion events, and work to explore the possibly non-linear effects of propeller flow pattern on the likelihood of entanglement.

14. SUBJECT TERMS
unmanned underwater vehicle, UUV, entanglement, eelgrass, kelp, micro-UUV, REMUS, underwater vehicle, marine vegetation, asymmetry, Disposable Reusable Expeditionary Warfare Underwater Vehicle, DREW UV

15. NUMBER OF PAGES
95

16. PRICE CODE

17. SECURITY CLASSIFICATION OF REPORT	**18. SECURITY CLASSIFICATION OF THIS PAGE**	**19. SECURITY CLASSIFICATION OF ABSTRACT**	**20. LIMITATION OF ABSTRACT**
Unclassified	Unclassified	Unclassified	UU

NSN 7540-01-280-5500

Standard Form 298 (Rev. 2-89)
Prescribed by ANSI Std. 239-18

THIS PAGE INTENTIONALLY LEFT BLANK

Approved for public release. Distribution is unlimited.

ASYMMETRIC INFLUENCE OF SINGLE PROPELLER UUV OPERATIONS ON ENTANGLEMENT WITH MARINE VEGETATION

James M. Dubyoski
Lieutenant, United States Navy
BS, United States Naval Academy, 2016

Submitted in partial fulfillment of the
requirements for the degree of

MASTER OF SCIENCE IN SYSTEMS ENGINEERING

from the

NAVAL POSTGRADUATE SCHOOL
June 2022

Approved by: Joseph T. Klamo
Advisor

Anthony G. Pollman
Co-Advisor

Oleg A. Yakimenko
Chair, Department of Systems Engineering

THIS PAGE INTENTIONALLY LEFT BLANK

ABSTRACT

This thesis continues previous work conducted on the interactions between a single propeller unmanned underwater vehicle (UUV) and marine vegetation. It attempts to define the asymmetric behavior of entanglement between a single, shroud-less propeller and synthetic eelgrass. A Disposable Reusable Expeditionary Warfare Underwater Vehicle (DREW UV), designed as a low-cost testing vehicle, was fixed at various test conditions in a towing tank. A four-factor full factorial design of experiments that varied lateral separation, depth, vehicle speed, and whether the eelgrass was on the port or starboard side of the vehicle was used to evaluate how these factors changed the likelihood of entanglement with a single strand of eelgrass. Each factor's impact was assessed as it pertained to which side of the vehicle the eelgrass was on. The tests revealed that significant asymmetry exists in the behavior of entanglement for a single propeller UUV based on the side of passage. The likelihood of entanglement is further reduced or increased based on the other variable factors. Thus, the asymmetry that exists does so on a scale. Certain test conditions can exacerbate this asymmetry and should be given consideration when applied to operational usage. Future work includes further testing to increase fidelity in results, testing to understand the stochastic nature of occlusion events, and work to explore the possibly non-linear effects of propeller flow pattern on the likelihood of entanglement.

THIS PAGE INTENTIONALLY LEFT BLANK

Table of Contents

List of Figures

THIS PAGE INTENTIONALLY LEFT BLANK

List of Tables

THIS PAGE INTENTIONALLY LEFT BLANK

List of Acronyms and Abbreviations

AUV autonomous underwater vehicle

DOD Department of Defense

DOE design of experiments

DREW UV Disposable Reusable Expeditionary Warfare Underwater Vehicle

GUI graphical user interface

ISR intelligence, surveillance, and reconnaissance

NPS Naval Postgraduate School

NSWC PC Naval Surface Warfare Center Panama City

ROV remotely operated vehicle

USN U.S. Navy

UUV unmanned underwater vehicle

THIS PAGE INTENTIONALLY LEFT BLANK

Executive Summary

As emphasis on unmanned systems increases through a variety of domains, the Department of Defense is not alone in its pursuit and proliferation of such technology to augment its traditional manned forces. Naval operations in the littoral waters present a key opportunity for such technology to provide critical assistance to ensure safe and effective operations. These areas are littered with low cost adversarial mines that can inflict costly damage on U.S. forces abroad. One such counter to this threat are unmanned underwater vehicles (UUVs) used to discover and neutralize enemy mines. However, UUV operations in littoral waters are often hampered by marine vegetation such as giant kelp and eelgrass that cause entanglement with the vehicle propellers.

Much has been done to explore the design of propellers from an efficiency point of view. Little, however, has been documented on the interactions between UUV propellers and marine vegetation. This study looked specifically at the influence of a single propeller UUV on a single strand of eelgrass in an attempt to determine whether asymmetry existed in the likelihood of entanglement based on the location of the eelgrass with respect to the vehicle. In this study, vehicle depth, speed, lateral separation from eelgrass, and the side by which the vehicle passes were varied to understand the changing likelihood of entanglement events with respect to each.

For this design of experiments, a small UUV designed and produced by the Naval Surface Warfare Center in Panama City, Florida was held at fixed intervals of each variable in a towing tank as the vehicle transited in the tank with the propeller's shroud removed. To remove the effects of the hull of the vehicle on the eelgrass, the vehicle transited in reverse. By doing so, the interactions between only the propeller and the eelgrass could be observed and entanglement events recorded.

In comparing the results from the tests run with the eelgrass on each side of the vehicle, there appears to be a significant difference in the likelihood of entanglement for a single propeller. With the vehicle operating in reverse, the propeller spins in a counter-clockwise direction as it approaches the eelgrass. When the vehicle passes with the vegetation on its right side, entanglement consistently occurs at greater distances than with the vegetation

on the left. This suggests that there is significant correlation between the direction of the propeller rotation and the location of the eelgrass. Furthermore, the study showed certain speed ranges were more susceptible to entanglement. In the most vulnerable positions, with the eelgrass on the vehicle's right side, the lateral separation between half of one and one propeller diameter, and the middle depth tested of 20 inches above the base of the eelgrass, testing showed the highest likelihood of entanglement at the slowest speeds. Additionally, entanglement instances decreased when speeds ordered reached 1.85 m/s, increased again at 2.05 m/s ordered, and then dropped again significantly as speeds continued to increase. This suggests a possible correlation between the ordered angular speed and the resultant flow pattern created as it pertains to the likelihood of entanglement.

Future continuation of this study may further explore the flow pattern created by propellers and their influence on the likelihood of entanglement. Much has been done to analyze and model the flow patterns of propellers and the changes that occur as angular speed varies. These patterns and their relation to influence caused on surrounding vegetation may offer a glimpse into what causes entanglement and provide an avenue to develop common operating procedures for UUVs in littoral waters.

Acknowledgments

I would like to thank my thesis advisors, Dr. Klamo and Dr. Pollman, for the expertise, guidance, and time provided on this thesis. Without their help, this thesis would not be possible. Thank you to Dr. Cameron Matthews and Mr. Brandon Davis at NSWC Panama City for providing distance support to get the vehicle setup. I would like to give a special thank you to my wife, Julia, my daughter Adelei, and my son Owen, for their love and support through the long hours spent troubleshooting, testing, and writing that made this possible.

THIS PAGE INTENTIONALLY LEFT BLANK

CHAPTER 1:
Introduction

This thesis explores the entanglement effects of marine vegetation on a single propeller unmanned underwater vehicle (UUV). The study utilizes the Disposable Reusable Expeditionary Warfare Unmanned Underwater Vehicle (DREW UV), a low cost unmanned underwater vehicle produced by Naval Surface Warfare Center Panama City to continue previous work on interactions of propellers and marine vegetation. It looks specifically at the asymmetric behavior of entanglement for a single, shroud-less thruster and its interaction with a single strand of eelgrass.

1.1 Background

The use of unmanned underwater vehicles (UUVs) in littoral waters presents unique advantages as well as challenges to the Department of Defense. While adversarial mines litter waters in contested areas, the use of UUVs provides significant means for disposal teams to locate and neutralize threats to U.S. forces [1]. In 2004, the Department of the Navy released its updated "UUV Master Plan." While much has changed since its release, the principle pillars driving the vision have not; these include: Intelligence, Surveillance, and Reconnaissance (ISR), Mine Countermeasures, Payload Delivery, and Information Operations [2]. Undertaking these missions would further the use of "unmanned vehicles as force multipliers and risk reduction agents for the Navy" in hard to reach and defended areas often "denied to traditional maritime forces" [2]. Often, these denied areas are coastal waters that possess known beds of vegetation to include giant kelp and eelgrass that pose a significant threat to the operation of underwater vehicles in the littoral environment. Specifically, eelgrass presents a significant threat to UUV operations due to the propensity of its strands to wrap around propellers and their hubs [3], [4]. Prolonged UUV operation relies on their ability to remain mission capable and uninhibited. The Navy in particular has a vested interest in lengthening the amount of time required between human interactions as it relates to UUV operation to maximize the risk reductions to its agents [5]. Understanding causes of entanglement and the resulting actions that can be taken to reduce occurrences could provide lengthened and sustained autonomous operations for these vehicles in support of

DOD missions.

1.1.1 Marine Vegetation (Eelgrass)

Figure 1.1. Example of Dense Wild Eelgrass. Source: [6].

Eelgrass, formally known as *Zostera marina* [7], provides a habitat rich in nutrients and diverse in function. This vegetation serves as a home to various sea creatures, filters sediment, reduces erosion, and performs many other vital functions within its ecosystem [8]. Its long strands, reaching up to 1.2 meters (4 feet) in length as seen in Figure 1.1, also provide mechanisms for storing greenhouse gases such as carbon dioxide [8], [9]. Known beds of eelgrass proliferate coastal waters across the globe as seen in Figure 1.2. As such, its conservation and growth in littoral environments are priorities for marine habitat managers worldwide. While they present difficult operating environments for underwater vehicles, their removal would cause severe detriment to their ecosystems and threaten devastating environmental effects [10].

Figure 1.2. Eelgrass Beds Shown in Green Around the World. Source: [10].

1.1.2 Survey of Propulsion Types and Propellers

Figure 1.3. Blue Robotics T200 Thruster Used by DREW UV. Source: [11].

Underwater vehicles differ from each other in numerous design aspects including shape, size, and propulsion type. This thesis is particularly interested in propellers and their entanglements with marine vegetation. While this study does not explore different types of propulsion, the selected propeller offers a look into the interactions caused by a commonly used product in underwater vehicles in the Blue Robotics T200 Thruster shown in Figure 1.3. A study conducted by LCDR Irgens utilized a REMUS 100 pictured in Figure 1.6. This

vehicle operated with an open, three bladed propeller that measured a blade diameter of 11.43 centimeters (4.5 inches) as seen in Figure 1.4 [3]. This larger propeller represents the more traditional understanding of underwater propulsion. The T200, however, is much smaller and provides significant propulsive power, but its likelihood of entanglement may differ greatly due to its reduced size, shrouded nature, and altered blade shape. Regardless of their

Figure 1.4. REMUS 100 Three-Bladed Propeller without Shroud. Source: [3].

differences, these propellers both offer substantive risk of entanglement due to their rotating nature and protruding blades. These characteristics also increase cavitation and noise, all of which produce undesired consequences when conducting DOD operations [12]. These problems have led to research and proposals for water jet propelled systems such as the autonomous underwater vehicle (AUV) in Figure 1.5. With solutions like these still on the horizon, traditional propulsion remains firmly planted in the operating picture. In March, 2022, the U.S. Navy selected the REMUS 300 as their next generation small UUV [13]. Coupled with the production from the Naval Surface Warfare Center of the DREW UV, the near future will heavily incorporate small, open bladed propellers as UUV usage in the littoral waters expands. Thus, this study chose to expand on LCDR Irgens' study of an open bladed propeller by removing the shroud from the T200 and exploring its interaction with marine vegetation.

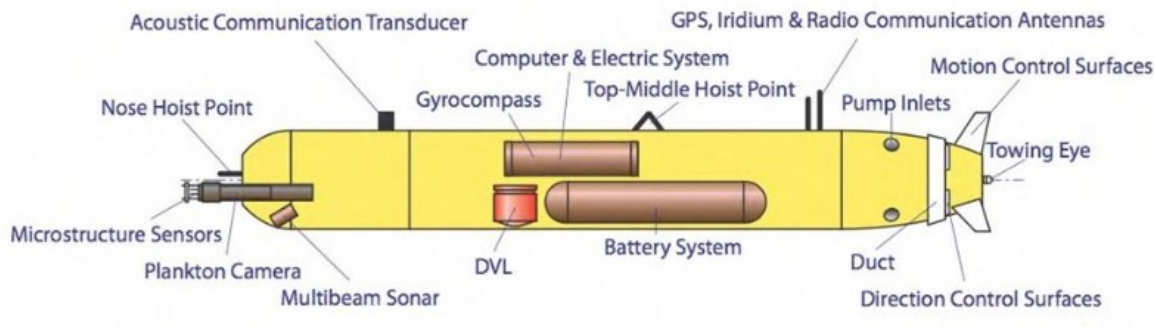

Figure 1.5. Proposed Water Jet Propelled AUV. Source: [14].

1.2 Previous Work

Very little research exists in the open literature on the entanglement likelihood and interactions of a propeller with eelgrass. Most research conducted in the environment explores the design of propellers in terms of efficiency [15], [16]. However, previous studies conducted by LCDR Irgens and LT Anuat at the Naval Postgraduate School explored the likelihood of entanglement for two different designs of underwater vehicles. Studying numerous factors, their work included the influence caused by the vehicle's body on different types of marine vegetation. LCDR Irgens' thesis used the REMUS-100 vehicle, pictured in Figure 1.6. This vehicle has a torpedo shaped hull and a large propeller. Her work included looking at the interactions between the REMUS-100 and various types and densities of vegetation. In varying the density, type, and placement of the vegetation, as well as the speed and direction of the vehicle's travel, she bounded the experimental space and explored the interconnected nature of these variables. Ultimately, her experiments suggested a higher likelihood of propeller entanglement with eelgrass then the other marine vegetation tested in her study, giant kelp. She also concluded there is a correlation between direction of travel and lateral separation of the vehicle from the vegetation and the likelihood of entanglement [17].

Figure 1.6. REMUS100 UUV Utilized in LCDR Irgens' Study. Source: [4].

Furthering that work, LT Anuat utilized a box-shaped remotely operated vehicle (ROV) produced by Blue Robotics shown in Figure 1.7. Her study used a vehicle with a different shape to explore the effects of geometry and the rotational freedom of the ROV's propellers. While concurring that speed and vegetation density and type were factors in entanglement likelihood, she also concluded that the vehicle's shape affected the interaction between the UUV and the vegetation [4].

Figure 1.7. Blue Robotics BlueROV2. Source: [4].

In both LCDR Irgens' and LT Anuat's previous studies, results indicated that characteristics such as vehicle shape, propeller design, vegetation type and density, and direction of vehicle travel affected the resultant likelihood of entanglement [3], [18]. LCDR Irgens also concluded that stern control surfaces affect the likelihood of entanglement and often result in a reduction in entanglement events [17]. She also performed preliminary tests that resulted in a limited data set suggesting asymmetry exists. There appeared to be a difference in the likelihood of entanglement between the propeller and eelgrass based on the side the

vehicle passed on. When passed on one side, the eelgrass tended to pull over the top and then wrap around the propeller. On the other side, the vegetation appeared to be pushed down, underneath, and then up around the propeller. These initial results are presumably a consequence of the single propeller design that creates the conditions shown in Figure 1.8 These initial results provided the basis for the experiments conducted in this study.

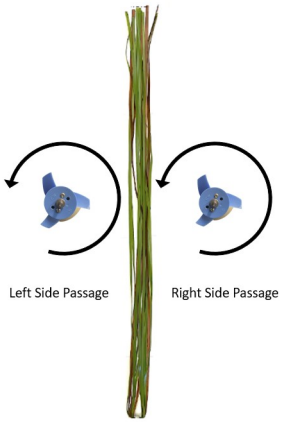

Figure 1.8. Demonstration of Single Propeller Asymmetric Interactions

1.3 Motivation and Objective

While previous work focused on determining the factors that lessen or increase the likelihood of entanglement, this study focused on the science of asymmetric entanglement rather than the operational considerations of entanglement. Specifically, this test attempted to reduce the variables under examination to only those related to the interaction between a propeller and marine vegetation. Therefore, the test design—while not strictly practical in real world execution—removed additional vehicle and environmental characteristics which may cause influence on the eelgrass. In continuing the work started by LCDR Irgens, this thesis attempted to scientifically define the asymmetric behavior of entanglement for a single propeller UUV. By conducting tests at varied conditions of lateral separation, vehicle speed, and depth, the study explored the changing shape of this asymmetry across the various test conditions. Defining the science of this behavior and understanding how factors change this behavior could lead to updates in vehicle design and operational considerations.

THIS PAGE INTENTIONALLY LEFT BLANK

CHAPTER 2:
Facilities and Equipment

This chapter discusses the facility and equipment utilized for this study. The test facility and equipment were located in the Hydrodynamics Laboratory in Halligan Hall at the Naval Postgraduate School. The test utilized a towing tank for operating a DREW UV with varying speeds as it passed a single strand of eelgrass. While both giant kelp and eelgrass plants are found in littoral operating areas, eelgrass often presents the most significant threat for propeller entanglement. As such, only eelgrass was used for this experiment, secured to a plate, and observed as the vehicle passed it at varying conditions.

2.1 Towing Tank

Figure 2.1 shows the test venue for this thesis, a towing tank that measures 10.97 meters (36.0 feet) long, 0.9144 meters (3.0 feet) wide, and 1.219 meters (4.0 feet) in height. The tank, constructed of aluminum, contains plexiglass panels along one side for viewing underwater events. The towing tank was filled to a depth of 0.9652 meters (38.0 in). This depth ensured that the water covered the full 0.9144 meters (3.0 feet) of the eelgrass as well as the height added by the plate used to secure the eelgrass. For this study, the water depth was set such that the eelgrass was fully emerged to reduce the variance in the eelgrass's position or tendency to entangle based on the tops of the vegetation folding over to one side. Filling the tank to this depth produced more consistent eelgrass positions for each test run. Two rails affixed to the top of the towing tank allowed a carriage to traverse the length of the tank. This carriage, a 1.905 cm ($\frac{3}{4}$ in) thick plate made of aluminum, glided on top of the rails and served as the attachment point for the vehicle's adapter and vertical sting.

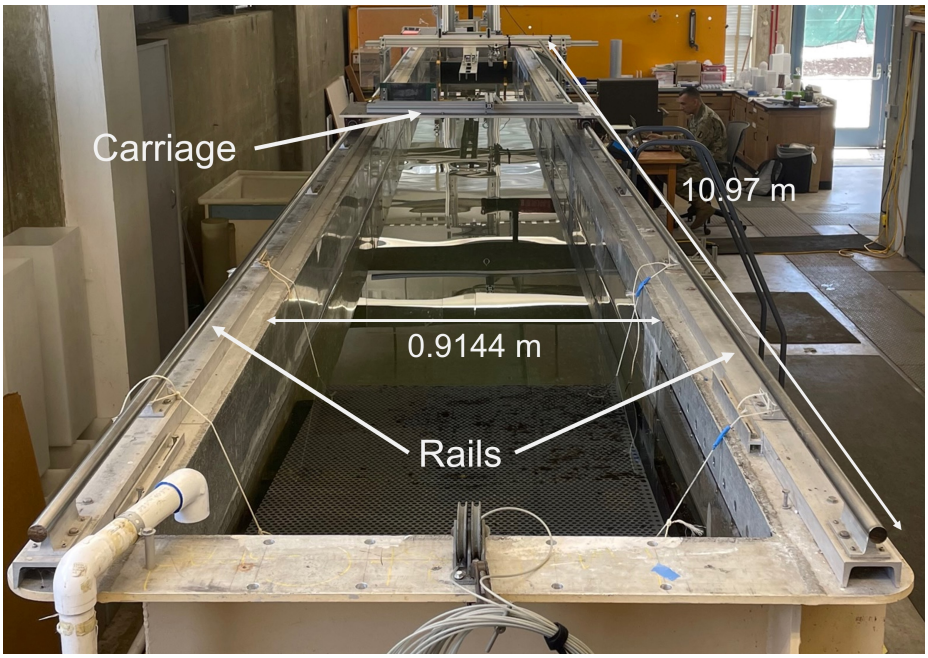

(a) Tow Tank End View

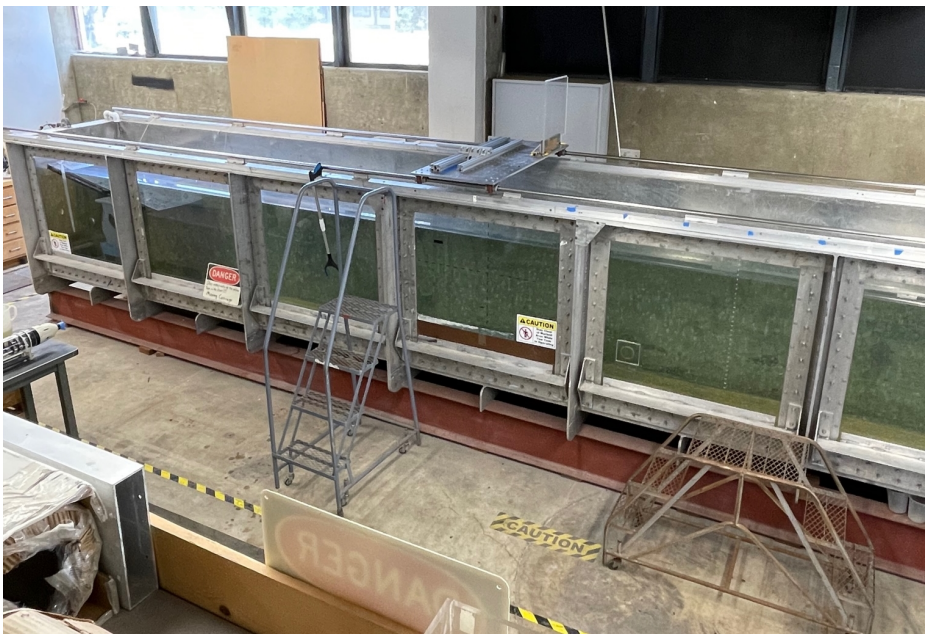

(b) Tow Tank Side View

Figure 2.1. Pictures of Testing Tow Tank Showing Dimensions and Carriage Assembly

2.2 Test Fixture

Figure 2.2 shows a top view of the carriage utilized to stabilize the UUV. This design allowed for the self-propulsion of the vehicle while restricting its roll, pitch, yaw, heave, and sway. It also fixed the vehicle's depth without requiring use of the vehicle's aft fins which allowed for very repeatable runs. On the aluminum carriage, two pieces of secured 80/20 T-slotted aluminum provide securing points for a perpendicular piece of 80/20. This is denoted as the movable sting support bar in the figure. This perpendicular piece could be secured at various marked distances that represented the lateral separation of the vehicle from the eelgrass. A single, double-wide 90-degree bracket, denoted as the lateral separation marker, was fixed to this perpendicular bar in between the carriages rails. This bracket provided a marker for the apparatus's relative position to the eelgrass. Two 90-degree brackets fixed

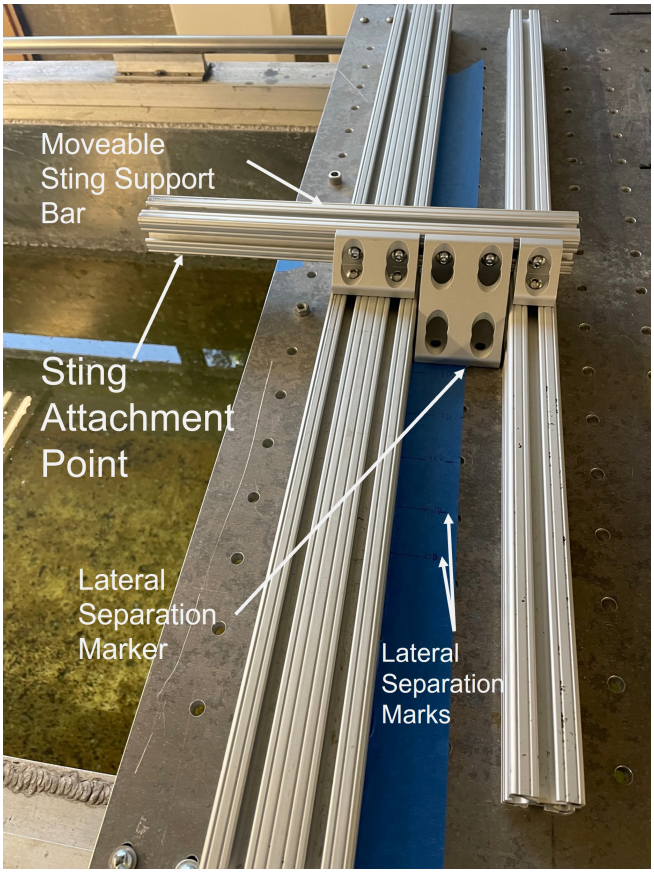

Figure 2.2. Carriage Top View Showing Assembly Pieces and Example Lateral Separation Marks

to a vertical sting with separation equal to the width of a single piece of 80/20 allowed the vehicle, adapter, and sting assembly to slide onto the free end of the perpendicular bar as shown in Figure 2.3(b). At shallow and deeper depths, altered configurations provided the necessary support given their location on the sting as shown in Figures 2.3(a) and 2.3(c) respectively. Below the shallow depth bracket, a single larger 90-degree bracket was used as an attachment point during mission upload. This placement on the sting ensured the mast of the vehicle was not submerged during the package upload and provided time to setup each test prior to severing communications with the vehicle.

Once both securing brackets were slid into the T-slots of the perpendicular bar, their bolts were secured. The sting itself consisted of 34 evenly spaced holes with 2.54 cm (1.0 in) of separation between each, measured 1.16 m (45.5 in) long, 2.54 cm by 2.54 cm (1.00 in x 1.00 in) in width, and contained two 0.635 cm ($\frac{1}{4}$ in) holes spaced 3.18 cm (1.25 in) on-center where the vehicle's adapter attached.

The adapter connecting the sting to the vehicle was designed to provide a secure attachment point for the vehicle while reducing the drag it added to the vehicle and test fixture. It was 3D printed based on the designs in Figure 2.4 and utilized two 1.27 cm (0.50 in) banding clamps to secure the vehicle to the adapter. Two 5.08 cm (2.00 in) long 0.653 cm ($\frac{1}{4}$ in) bolts were used to secure the adapter to the sting.

The banding clamps were fed through the slots in the adapter and around the body of the vehicle. The clamps were tightened firmly to prevent rotation of the DREW within the adapter as shown in Figure 2.5. This combination of the vehicle, the adapter, and the sting is referred to in this thesis as the vehicle assembly.

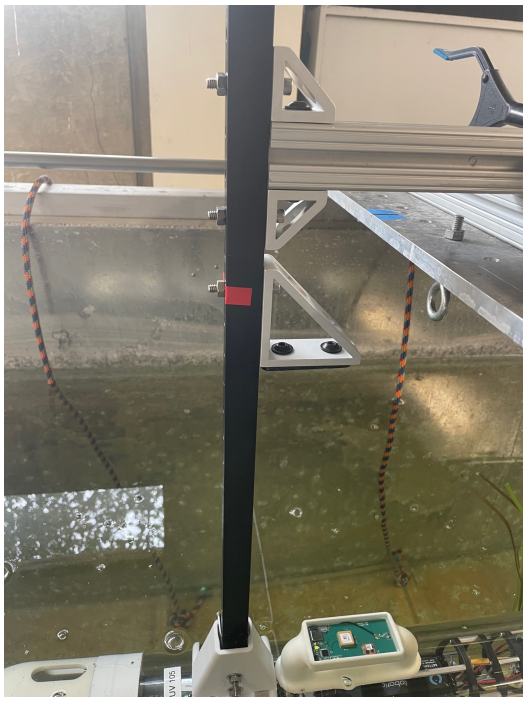

(a) Shallow Depth

(b) Medium Depth

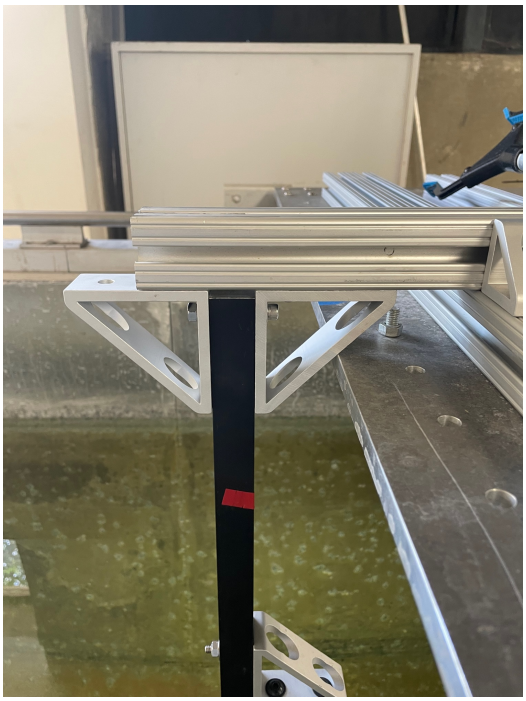

(c) Deep Depth

Figure 2.3. Different Depth Settings On Sting Shown Installed On Carriage Assembly

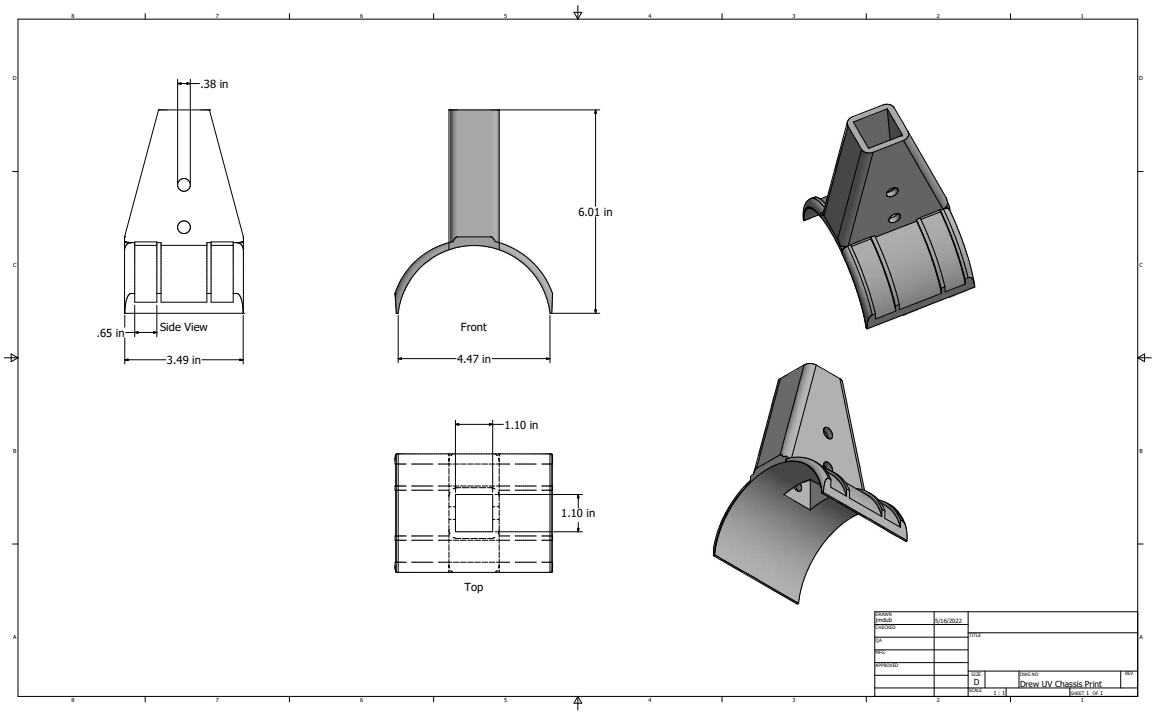

Figure 2.4. DREW UV Adapter Engineering Drawings Used for 3D Printing

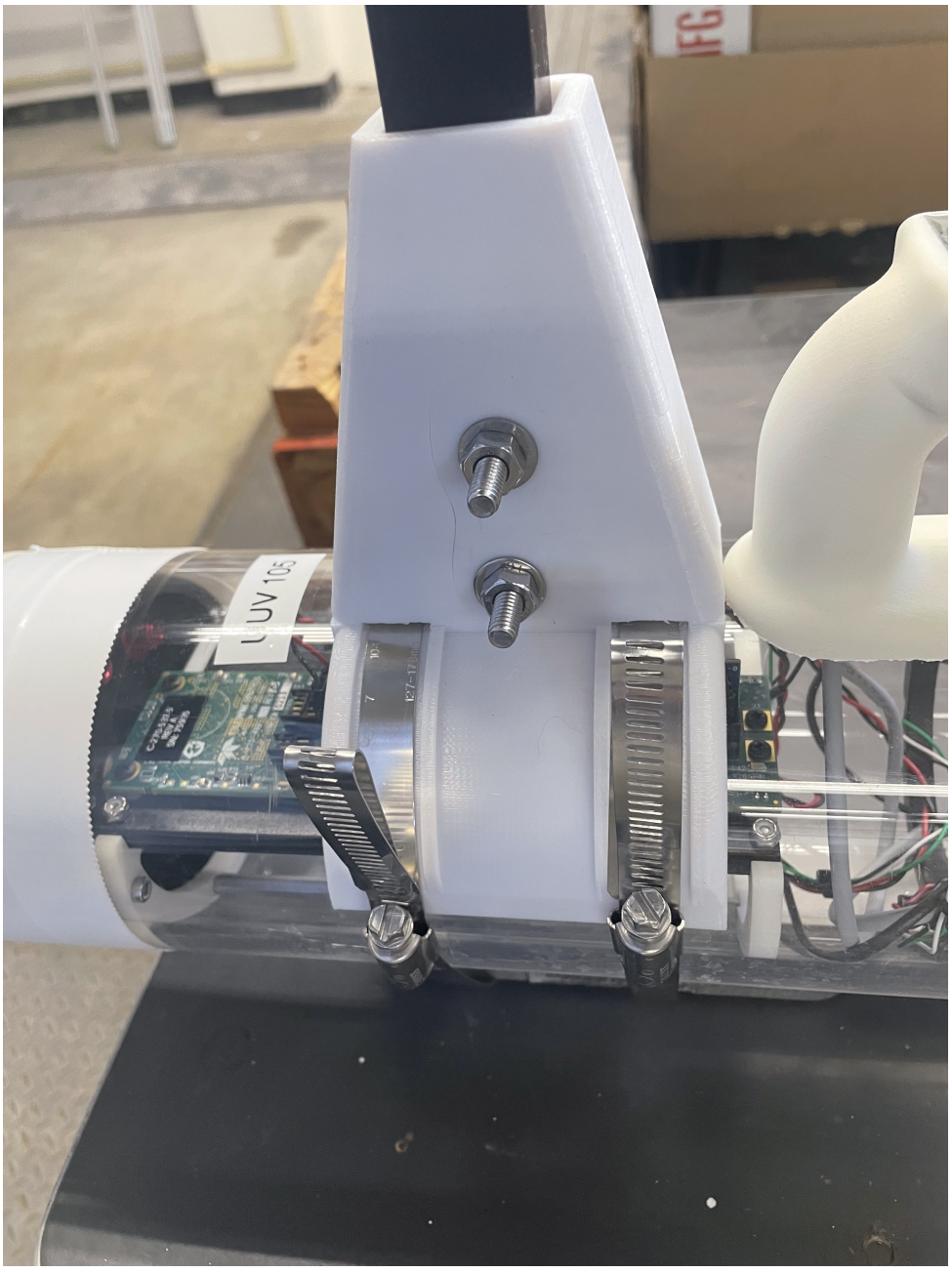

Figure 2.5. DREW UV Adapter Installed with Banding Clamps

2.3 DREW UV

The DREW UV, pictured in Figure 2.6, is a low-cost unmanned underwater vehicle capable of waypoint navigation, payload delivery, and group or swarm operation [19]. Developed and produced by the Naval Surface Warfare Center in Panama City, Florida, this vehicle was the only UUV used for testing in this study. It measures 0.965 m (38.0 in) long, 11.43 cm (4.5 in) in diameter, has a conical nose and a tapered aft end, three aft fins for vehicle control, and a T200 thruster produced by Blue Robotics for propulsion. For this experiment, the shroud encompassing the propeller was removed and the overall length of the vehicle reduced to 0.946 m (37.25 in). The diameter of the propeller measures 7.62 cm (3.00 in). Additionally, to eliminate any influence they may have caused on observed interactions, the vehicle's aft fins were removed. This helped to ensure that the interactions were isolated to those between the vegetation and the propeller.

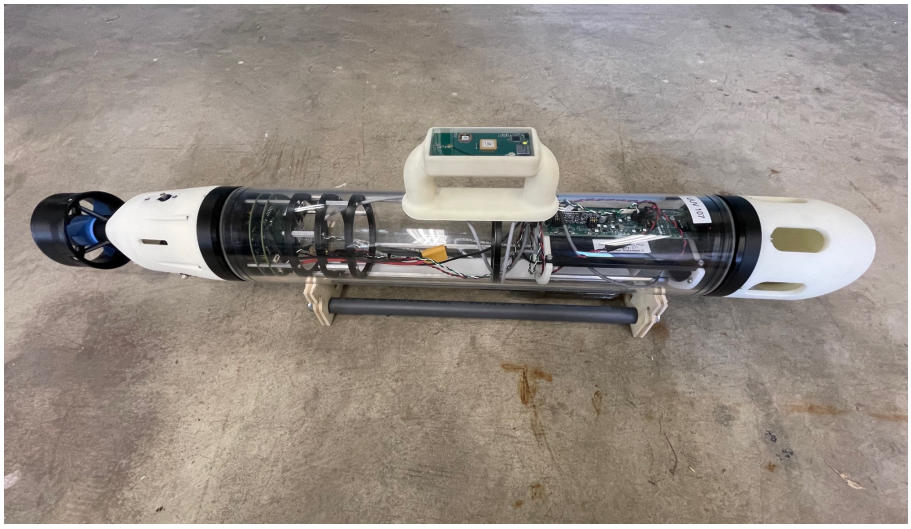

Figure 2.6. DREW UV Shown with Shroud Installed and Fins Removed

2.4 GUI

Due to the untethered design of the DREW UV, each set of tests was translated into a mission package to be uploaded to the vehicle. Once the mission was uploaded and started, the vehicle was submerged and placed into position for testing. The graphical user interface utilized to accomplish this mission was launched following a series of steps outlined Appendix A.

Once started, the user could connect to the vehicle, upload a mission package, and begin the mission from the screen shown in Figure 2.7(a). While connected, the user can also monitor the vehicle's status from the status panel as shown in Figure 2.7(b).

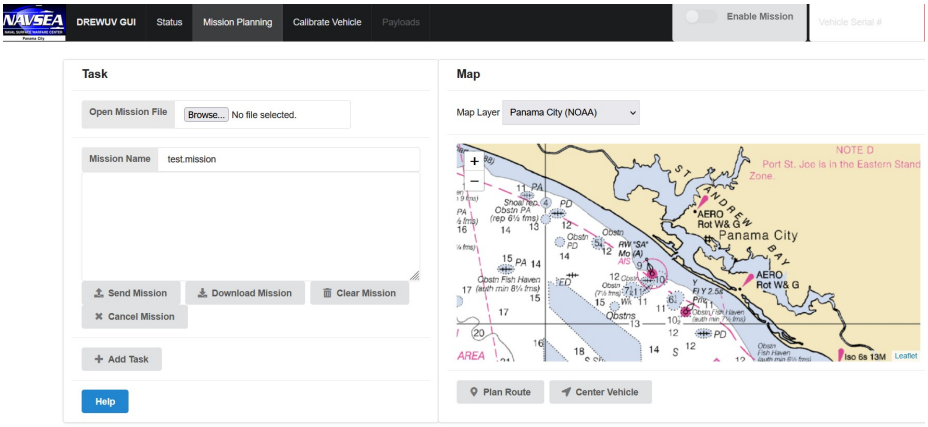

(a) Mission Planning

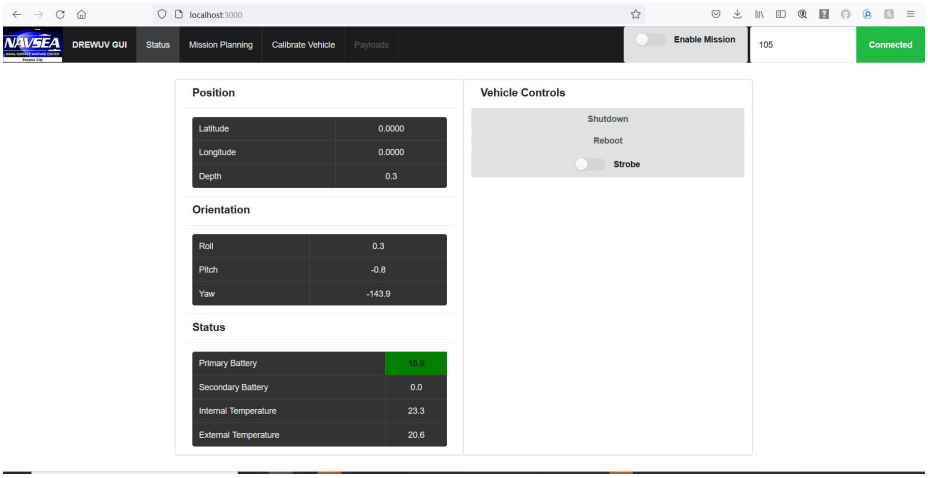

(b) Status Page

Figure 2.7. Graphical User Interface Showing Mission Planning and Vehicle Status Pages

To connect to the vehicle, the GUI required a Microhard PDDL2450, a miniature data link capable of connecting the operator's laptop to the vehicle. The Microhard was connected via its LAN port by ethernet cable to the laptop as shown in Figure 2.8. A static internet protocol address was configured on the host laptop and a local host node started. These

setup procedures are further detailed in Appendix A.

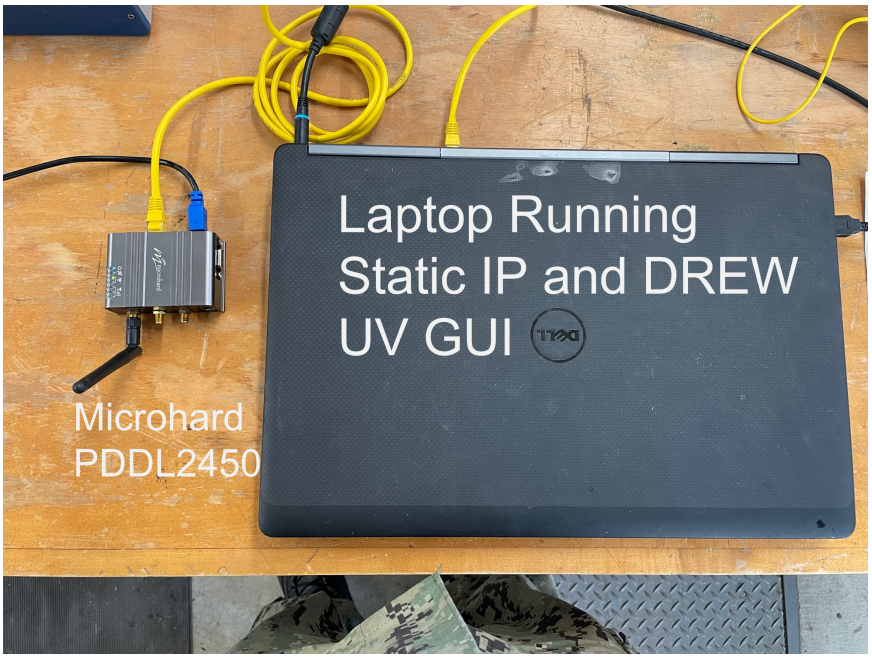

Figure 2.8. Modem and Laptop Setup Used to Run GUI

2.5 Marine Vegetation

This thesis focused on the interaction between the propeller and a single strand of eelgrass. For the purpose of this experiment, a single strand of eelgrass is described as one bundle of eelgrass with a single attachment point on the plate shown in Figure 2.9.

Each bundle is made up of 20 individual strands measuring 91.44 cm (36 in) in length and will be referred to as a single strand in this thesis. The eelgrass utilized in this study is synthetic and mimics the characteristics of that often found in littoral waters. Shown in Figure 2.10, these bundles of eelgrass were characterized in LCDR Irgens' thesis. From this characterization, she came to two major conclusions. First, the eelgrass was able to wrap around a cylinder with a diameter as small as 0.8 ± 0.03 cm ($\frac{5}{16}$ ± $\frac{1}{128}$ in)—a diameter smaller than both the REMUS and the DREW's propeller hub. Second, she found that the eelgrass was not able to support its own weight when the eelgrass was cantilevered more than 15.24 cm (6 in).

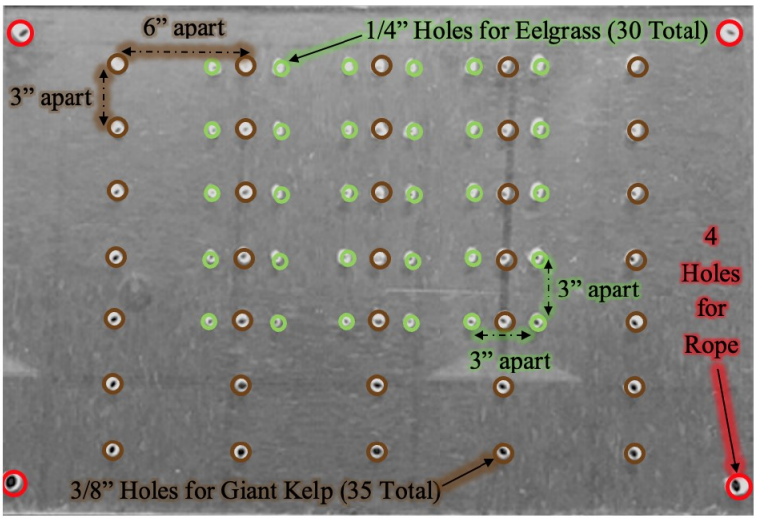

Figure 2.9. Vegetation Plate Source: [4]

While the centerline holes in Figure 2.9 are marked for use with synthetic giant kelp, they were used for this experiment with the sole addition of a washer to secure the eelgrass to the plate. This plate was then lowered into the tank with four ropes connected at the plate's corners.

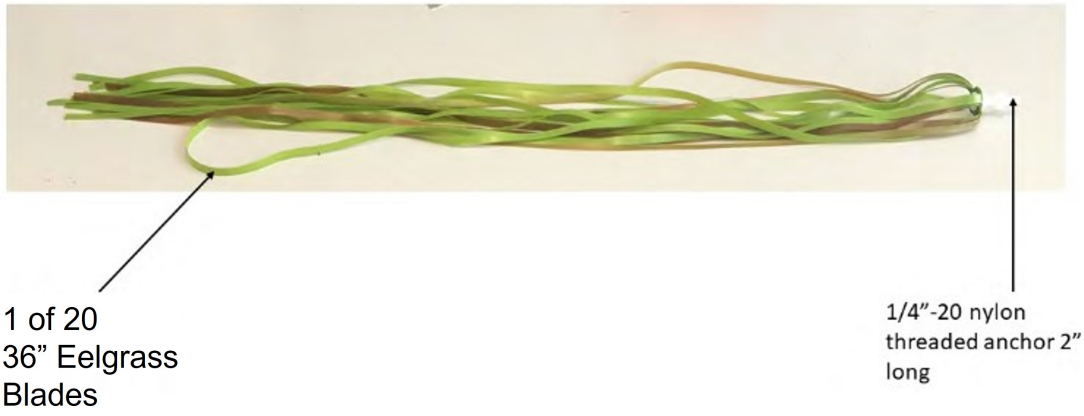

Figure 2.10. Example Synthetic Eelgrass Strand Used for Study. Adapted from: [3].

CHAPTER 3:
Design of Experiments and Test Procedures

3.1 Methodology and Approach

This study aims to determine if an asymmetric relationship exists between a single propeller and the likelihood of entanglement with marine vegetation. If such a relationship exists, the hypothesized variables contributing to the resultant difference in likelihood might include different propeller speeds, lateral separation, vehicle depth in relation to the vegetation, and the side the vehicle passes the vegetation on. These variables create the bounds for the design of experiments described later in this chapter. Therefore, the study is designed to hold all variables steady while incrementally changing a single variable for a given number of runs. For each run, the amount of influence caused on the eelgrass by the propeller as well as entanglement events were recorded. For a given test condition, ten test runs were performed and results recorded. Due to the stochastic nature of entanglement and the inherent variation of the eelgrass condition between each run, many runs at each condition were performed to assess the likelihood of an entanglement event to occur.

3.2 UUV Pre-Dive Checks

The first step in readying the DREW UV for operation is to connect the lithium ion battery to power on the vehicle. This is done by removing the aft section of the vehicle from the main body. When inserting the battery, the miniature coaxial cable, or uFL connector, that connects the mast data to the main circuit board has a tendency to become disconnected. This cable's connection should be verified as secure to the receptacle labeled "main" on the vehicle's Microhard modem and marked by the arrow in Figure 3.1 labeled Mast Coaxial.

Taking care to clean the gaskets that provide the water tight seal, the aft end is then re-inserted into the main body. The junction points of the body at the forward and aft ends of the vehicle are then carefully wrapped a minimum of 1.5 times with Polyken 827 film tape as shown in Figure 3.2(a). This ensures that no water intrudes through the connection points of the vehicle. Lastly, the vehicles vent plug must be inserted and tightened as seen

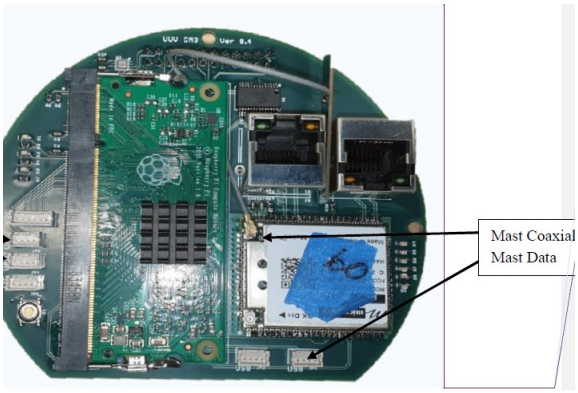

Figure 3.1. DREW Microhard UFL Connection. Adapted from: [19].

by the plug marked “OK” in Figure 3.2(b).

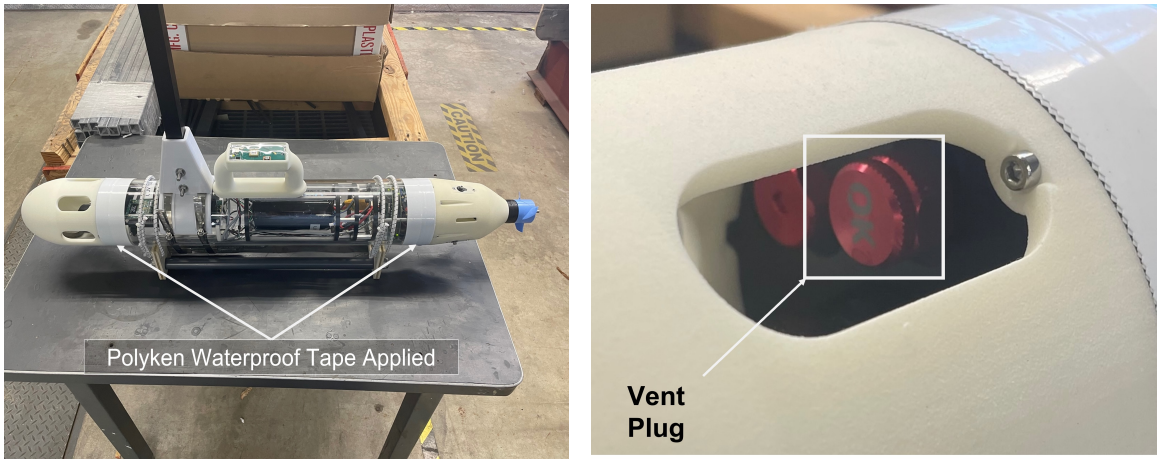

(a) Vehicle with Waterproof Tape Applied (b) Vent Plug Installed

Figure 3.2. Vehicle Fully Waterproofed

3.3 Experimental Setup

3.3.1 Carriage Assembly Setup

With the vehicle pre-dive procedures completed, the vehicle assembly was placed in the tow tank and attached to the carriage at the lowest bracket on the sting as depicted in Figure 3.3.

This ensured that only the vehicle's mast was protruding from the water and could maintain connection with the laptop for mission upload. With the vehicle held in this position, it was not necessary to tighten the bolts to secure the bracket to the carriage assembly. Not doing so allowed for easier transition of the vehicle after mission package upload to the desired depth. The sliding lateral separation marker was then placed at the desired distance, marked in multiples of half-diameters, and the bolts securing the perpendicular bar to the rails on the carriage were tightened.

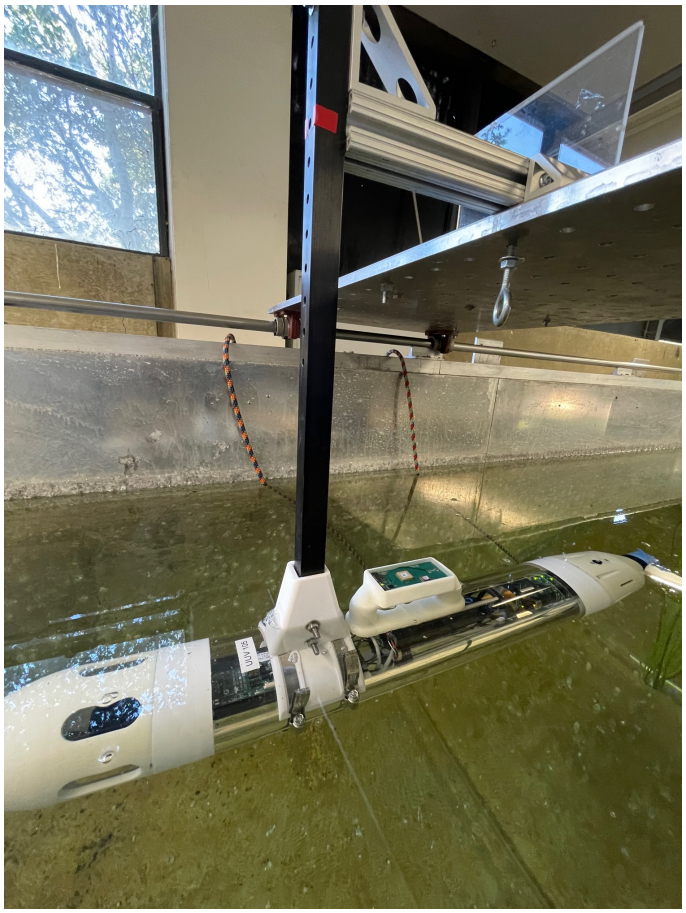

Figure 3.3. Vehicle Set at Shallow Depth

3.3.2 Vegetation Setup

A single strand of eelgrass was attached to the plate shown in Chapter 2. This strand was placed in the center of the plate and secured with a two inch long, quarter inch screw. The

plate was lowered into the tank such that the eelgrass was on the centerline of the tank. The eelgrass was combed to an upright position and given 90-seconds to settle. When ready for testing, the eelgrass appeared as it does in Figure 3.4. While variance exists in the eelgrass's position for each run, the same procedural steps were taken before each run and numerous runs were conducted at each condition. This allowed for the assessment of the likelihood of entanglement regardless of the inherent randomness of an entanglement event in each run.

Figure 3.4. Eelgrass Ready to Test

3.3.3 Vehicle Setup

When the vehicle and carriage assembly were setup, the mission package could be uploaded. In initial testing, mission packages were built at time of test to provide flexibility in reacting to initial results. However, for the design of experiments, full mission packages, containing multiple test conditions, were pre-built and uploaded at time of test to follow the design

of experiments test conditions covered later in this chapter. On the mission planning tab of the user interface, the add task option was selected. To allow time to submerge, secure, and align the vehicle prior to the first run, the first task added was a 90 second "Wait" task. A full description of the process for starting the user interface and building the mission packages can be found in Appendix A. Once the package was loaded into the GUI, the "Send Mission" option as described in Appendix A was selected. If successful, the "Send Mission" option illuminated in green. The mission was then enabled by toggling the switch in the upper right hand corner. With the mission package enabled, the vehicle was then lowered to the desired depth and fastened tightly via the bolts on the securing brackets. The carriage was then positioned 91.44 cm (36 in) in front of the eelgrass. In these tests, the vehicle travelled in reverse as it passed the eelgrass. Therefore, when placed in front of the eelgrass, the vehicle's propeller was closer to the eelgrass than its bow.

3.4 Exploratory Testing

With the experimental setup complete, exploratory testing provided a means for determining the applicable range of the variables in this study. After enabling the mission and lowering the vehicle, a clamp held the carriage fixed in a position where the vehicle's propeller was in line with, or 0.00 cm in front of, the eelgrass. The lateral separation was varied in 1.27 cm (0.50 in) increments, the vehicle was run for a cycle of 10 tests, starting with a one second run and increasing incrementally by one second. The first exploratory tests utilized a 30-second interval between runs. Successive iterations of this testing revealed that for longer duration runs, a 90-second wait period was required to allow the water in the tank to settle prior to the next run. Therefore, the design of experiments (DOE) utilized in Figure 3.5 for this testing used a wait period of 90-seconds between each run. The exploratory testing revealed that the 90-second wait period was sufficient for the tank to fully settle and should be used for the full DOE between each run.

This exploratory testing also provided a picture of the expected interaction between the vehicle propeller and the eelgrass. As the propeller rotation time increased and the lateral separation decreased, the different levels of influence were observed. These levels are classified in the following section on interaction taxonomy. The exploratory testing not only allowed for the bounding of variable extremes as discussed in Chapter 4, but for the

definition and delineation of the degrees of influence leading up to an entanglement event. The significance of these delineations is further discussed in Chapter 4.

Lat Dist / Time (sec)	0	0.5	1	1.5	1.75	2.5	3	3.5	4	4.5	5	5.5	6	6.5	7	7.5	8	8.5	9	9.5	10
1																					
2																					
3																					
4																					
5																					
6																					
7																					
8																					
9																					
10																					

Figure 3.5. Exploratory Testing DOE

3.4.1 Interaction Taxonomy

The amount of influence on the eelgrass caused by the propeller is not binary. The interaction occurs to varying degrees from none at all to entanglement, but also includes those events which occur in between. In this study with a single strand of eelgrass, a level of influence that does not amount to entanglement is operationally insignificant. However, it allows for scientific study of when interactions begin to occur, as well as the likelihood entanglement may occur given prolonged operation alongside the vegetation. As one might expect, conditions which often cause low amounts of influence also result in an almost negligible probability of entanglement. Those conditions which create moderate to high levels of influence also produce more entanglement events given a series of 10 runs at a given condition. Thus, Figure 3.6 depicts this study's classifications of the levels of influence as they pertain to the physical response of the eelgrass to the propeller's rotation. In each figure, the yellow line marks the initial position of the eelgrass. The orange line highlights the amount of reaction the eelgrass displays for each level of influence.

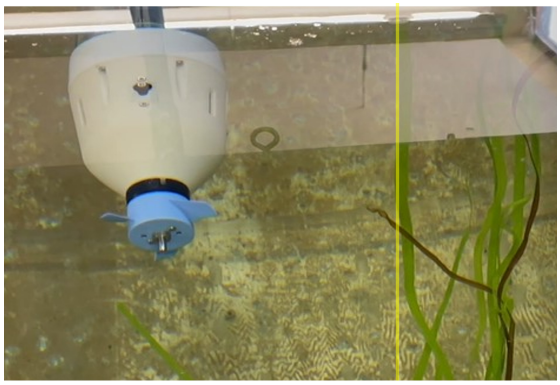

(a) No Influence

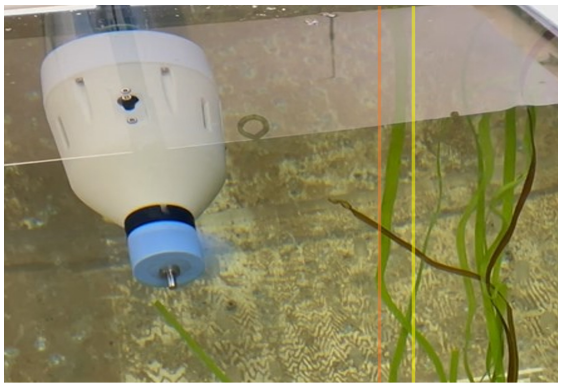

(b) Low Influence

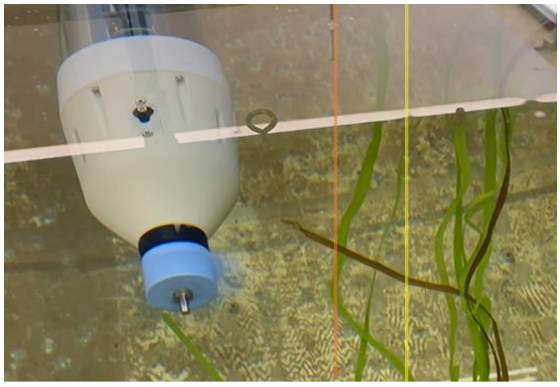

(c) Medium Influence

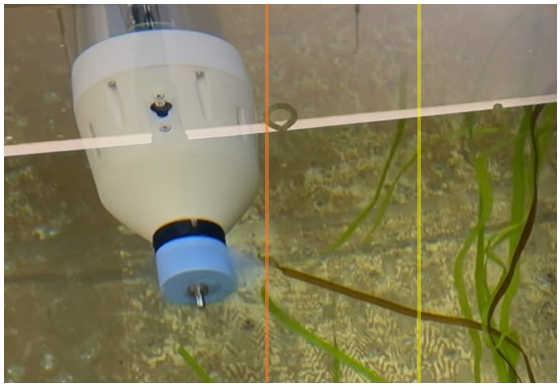

(d) High Influence

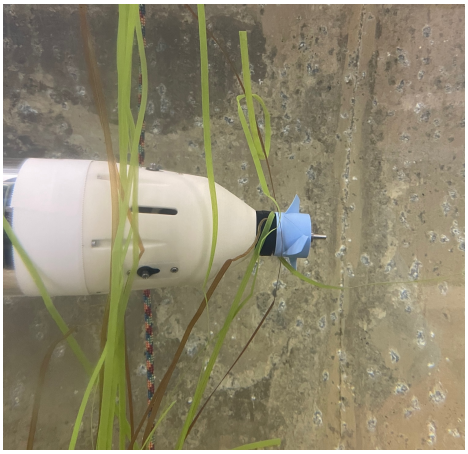

(e) Entanglement Event

Figure 3.6. Interaction Taxonomy

No Influence

The classification of "No Influence" was used when the vehicle passed by the eelgrass and no noticeable movement of the eelgrass towards the propeller was observed. With the vehicle moving backwards, the eelgrass is sucked towards the vehicle's hull after the propeller passes the eelgrass. This movement was not included in the classification of any level of influence. Figure 3.6(a) depicts the propeller in rotation and passing the eelgrass. In this instance, the eelgrass remains in its position until after the propeller blades have passed.

Low Influence

The "Low Influence" classification was used when little movement of the eelgrass was observed. The movement that occurred was clearly visible, but minimal with the eelgrass usually bending at the height of the propeller. However, this motion, as shown in Figure 3.6(b) did not threaten contact with the propeller or a likelihood of entanglement.

Medium Influence

The term "Medium Influence" was used in this taxonomy to denote a significant movement in the eelgrass as shown in Figure 3.6(c). While the movement was large and noticeable, the eelgrass did not contact the vehicle's propeller blades under this condition.

High Influence

In "High Influence" conditions, the eelgrass was influenced by the propeller to such a degree that the eelgrass contacted the propeller. However, this interaction did not cause the eelgrass to wrap around the propeller's blades or hub and the vehicle's motion is not slowed. In this instance, the eelgrass blades were deflected away. Still images, such as Figure 3.6(d) are difficult to capture this deflection, but the figure noted shows the eelgrass in such a position that deflection is imminent. During observation, this contact is obvious and easily differentiated from both medium influence, where no deflection occurred, and entanglement.

Entanglement and Occlusion

An "Entanglement" condition is one that prevents further operation of the vehicle. In this cases, the eelgrass wraps around the propeller's hub, shaft, or blades and slows the vehicle to

a stop. During entanglement events, pictured in Figure 3.6(e), the vehicle remains entangled even after the motor has shut down. This effectively results in a "mission kill" of the vehicle.

Occlusion events are those where eelgrass blades wrapped and, in most cases, slowed the progress of the vehicle. Yet, in occlusion events, the continued operation of the propeller broke the propeller free and the vehicle returned to an operable status, transiting further down the tank. These events are once again difficult to depict in still imagery, but begin similar to the events pictured in Figure 3.6(e) and end with an unobstructed vehicle.

3.5 Experimental Design and Procedures

3.5.1 Design of Experiments

This design of experiments (DOE) was intended to highlight any discernible difference in the likelihood of entanglement given the different sides of passage for the vehicle by the eelgrass. A test condition, for the purpose of this experiment, was a particular combination of values for each parameter of the DOE shown in Table 3.1. For instance, a set of 10 runs was conducted with the vehicle on the left side of the eelgrass, the speed set to -1.25 m/s, the lateral separation at two diameters, and the depth set to the middle setting of 50.8 cm (20 in). The next set of 10 runs would be conducted for the next interval of speed with all other variables remaining the same. Once every interval was complete for the vehicle's speed at these conditions, another variable would be iterated and the same process completed. This provided a four factor full factorial design of experiments. The intended result of this DOE was the ability to analyze the data for differences in each variable change and to determine if asymmetry exists based on the side of operation.

Table 3.1. Design of Experiments

# of Runs	10x		
Side	Left	Right	————————
Speed Range	Min:-1.25 m/s	Max:-2.35 m/s	Step: 0.1 m/s
Lateral Separation	Min:0.0D	Max:2.5D	Step: 0.5D
Depth†	Deep 12.7 cm (5.00”)	Middle 50.8 cm (20.0”)	Shallow 76.2 cm (30.0”)
†measured from bottom of eelgrass			

3.5.2 Procedural Steps

With the setup complete, the vehicle in position, and the eelgrass combed into position, the procedural steps for this experiment were relatively simple. Once the initial wait expired, the first ordered speed executed and the vehicle moved in reverse - propeller first - towards the eelgrass. As the vehicle passed the eelgrass, the influence on the eelgrass from the propeller was observed and recorded. If the vehicle entangled, the run was marked “E” for entangled. Otherwise, the amount of influence was noted and the vehicle manually moved back to its starting position.

Due to the lack of tethered communications with the vehicle, there was no mechanism to stop the propeller should it entangle. Thus, the vehicle run time for each run was limited to six seconds. This time proved enough to allow the vehicle to clear well past the eelgrass, but would not allow excessive motor run time and subsequent burnout should the vehicle entangle. With the vehicle reset, the eelgrass was again combed in an upright position. In initial testing, the prolonged operation of the propeller produced a noticeable effect in the tank that could be misconstrued as influence on the eelgrass. This was likely caused by a non-negligible amount of the water being moved in such a relatively small and confined tank and causing the water to recirculate. Therefore, a 90-second wait was programmed between each run at a given testing condition to allow the water in the tank to settle. After this time, the effects on the eelgrass had subsided and were assumed to be negligible. It also provided enough time to free the propeller should it become entangled with the eelgrass.

Once all ten runs for a given condition were complete, the vehicle was once again raised to the shallow setting, set to the next condition, and reloaded with the mission package. This process was repeated for every condition until all conditions had been tested.

THIS PAGE INTENTIONALLY LEFT BLANK

CHAPTER 4:
Results and Analysis

The goal of this study was to learn about entanglement events occurring with a single open propeller and determine if there exists some level of asymmetry in results. The results of the experiment present data that relates to these objectives. Additionally, certain outcomes from the study, while seemingly tangential, were worth noting or exploring further. Therefore, the analysis of these results notes the entanglement events as they relate to the varied conditions, highlights the differences due to asymmetry, but also presents preliminary analysis on levels of influence as described in the taxonomy in Chapter 3. The additional analysis may prove useful for future work stemming from this thesis.

4.1 Exploratory Testing Results

1.00 m/s Ordered Speed																					
Lat Dist (cm) / Time (sec)	0.00	1.27	2.54	3.81	5.08	6.35	7.62	8.89	10.16	11.43	12.70	13.97	15.24	16.51	17.78	19.05	20.32	21.59	22.86	24.13	25.40
1								H	H	M	M		L		N		N		N	N	N
2								E	E	M	M		L		L		L		L	N	L
3								E	E	E	H		M		L		L		L	L	L
4								E	E	E	H		M		M		L		L	L	L
5								E	H	H	H		H		M		L		L	L	L
6								H	E	H	H		H		M		M		L	L	L
7								E	E	E	H		H		H		M		M	L	L
8								E	H	E	E		H		H		M		M	L	L
9								H	H	E	E		H		H		H		M	M	L
10								H	H	H	H		H		H		H		H	M	L

Figure 4.1. Exploratory Test Results Showing Influence Levels and Entanglement with Vehicle Held Stationary

Figure 4.1 provides the DOE results for the exploratory testing. These results represent only part of the beneficial information obtained from these initial trials. In the follow-on full study DOE, the lateral separation was adjusted in relation to half-diameters of the vehicle's propeller. In this testing, the lateral separation was adjusted by 1.27 cm (0.50 in) intervals to start. Because this test was intended to provide the bounds for the study, some intervals were skipped when the fidelity was not necessarily crucial. Between 22.5 cm (9.00 in) and 12.7 cm (5.00 in) of separation, the change occurred in 2.54 cm (1.00 in) steps. This was due to the resulting pattern that emerges as the lateral separation decreases.

As evidenced by the results, the influence caused by the propeller gradually increases as the lateral separation decreases. However, once the vehicle's centerline is 12.7 cm (5.00 in) off-center from the eelgrass, the first indications of entanglement begin to occur. Therefore, with a stationary vehicle, entanglement began when the eelgrass was between 1.5 and 2 diameters of a propeller away from the vehicle centerline. This result informed the full DOE for unrestricted movement of the vehicle testing and bounded the lateral separation. To encompass all anticipated entanglement events, the full DOE included the 2 diameters of a propeller as well as an additional half-diameter.

As stated in Chapter 3 in the setup for exploratory testing, these tests also informed the required wait period between each test run. In initial testing, only 30-seconds separated each run. As the vehicle ran longer, possible forces created by the moving water in the enclosed tank began to effect the position of the eelgrass. Rather than bend at the height of the propeller, the eelgrass would begin to sway in one motion, regardless of the lateral separation if the run time was long enough. By increasing the wait time between test runs to 90-seconds, this swaying motion subsided prior to the next run. Furthermore, this testing revealed the different motions created by propeller influence versus the water movement in the tank and substantiated the assumption that further testing would not be critically influenced by the enclosed nature of the experiment. It can be reasonably assumed that entanglement events occurring in these experiments were attributed to the influence caused by the propeller and not additional forces created from the re-circulation of the water in the tank.

4.2 Unrestricted Movement Results

The exploratory testing results proved useful in understanding the limits of when entanglement events may occur and provided the bounds for the tests that followed. It also provided initial results of how the eelgrass is influenced by the propeller. However, when designing a system such as a UUV, one may be far less concerned with the categorization and study of influence than the likelihood of entanglement. System designs incorporate shrouds or enclosures to help reduce the occurrences of entanglement. Yet, studies of flow patterns and forces caused by the propeller often focus on propeller efficiency rather than the interactions with marine vegetation. Thus, the results for each set of test depths were separated into two

distinctive categories. The first shows solely the entanglement events that occurred for the given conditions. This allowed for the development of a likelihood of entanglement based on a binary understanding of the events - either the vehicle entangled or it did not.

The second set of results shows a qualitative visual representation of amount of influence caused on the eelgrass. To do this, an arbitrary scale from 0-1 was developed that provided a weight to each level of influence as shown in Table 4.1. These values do not correspond to a likelihood or probability. Instead, they are used to provide a means of averaging the ten tests run at each condition and a way to compare each condition by assigning values based on the significance of the interaction. Entanglement events, as in the quantitative results, were assigned a value of one, while no interaction received a value of zero. The varying levels of influence received values evenly spaced between those, with the exception of an occlusion event. These events, where the vehicle entangled and broke free, were assigned a value of 0.9. In this testing, there was no way to predict and no apparent pattern to when an occlusion event might occur vice an entanglement. Therefore, these interactions were weighted with a level of influence nearer that of an entanglement then of the "high" influence weight value. By pairing the taxonomy discussed in Chapter 3 with this weighted scaling, the qualitative results of the amount of influence produced in any given condition were produced for each section below.

Table 4.1. Weighted Taxonomy

Taxonomy	Abbr.	Weight
Entangled	E	1.00
Occluded	O	0.90
High	H	0.75
Medium	M	0.50
Low	L	0.25
None	N	0.00

4.2.1 Overall Results

The Design of Experiments run for this study produced telling evidence that asymmetry exists for the likelihood of entanglement. This likelihood is parsed and scrutinized further in the following sections. Looking at the overall results may be enough to say that asymmetry exists, as evidenced in Table 4.2. At each lateral separation interval, a total of 300 runs were conducted based on each speed tested and the three different depths. The table shows the vehicle entangled 269 times out of 300 runs conducted with the vehicle centerline. Most notably, the 0.5-1 diameter regions on each side show the largest contrast. Out of 300 runs conducted at 0.5D on the left side, 184 of them resulted in entanglement. The right side, however, only experienced 99 entanglement events over the same 300 runs.

Table 4.2. Entanglements by Lateral Separation

	Lateral Separation	Entanglements	Total (Side)
Left	2.5D	0	268
	2.0D	0	
	1.5D	2	
	1.0D	82	
	0.5D	184	
Centerline	0.0	269	
Right	0.5D	99	102
	1.0D	3	
	1.5D	0	
	2.0D	0	
	2.5D	0	

Still, the data received from these studies suggest that asymmetry is not the only significant factor that effects the likelihood of entanglement. In fact, the variation of certain factors may exacerbate effects caused by the asymmetric nature of a propeller's interaction with vegetation. For instance, Table 4.3 lists the total number of entanglements based on the various depths and speeds tested in this study. These results suggest there is a correlation between the vehicle's vertical position relative to the eelgrass and the likelihood of entanglement. The following sections explore these results to determine if a connection between

depth and the side of passage exists. Additionally, the test results indicate a significant factor on entanglement likelihood related to the vehicle's ordered speed. Like the changing depth, there appears to be a correlation between the speed and the side of vehicle passage. The cumulative evidence suggests that significant asymmetry exists in the likelihood of entanglement of a single propeller UUV based on the side of passage.

Table 4.3. Entanglements by Depth and Speed

Depth	Total Entanglements
Deep	246
Medium	276
Shallow	117
Speed	-
1.25	73
1.45	74
1.65	68
1.75	66
1.85	67
1.95	63
2.05	59
2.15	62
2.25	53
2.35	54

Figures 4.2(a) and 4.2(b) provide visual representations of the data in Table 4.3. They compare the number of entanglements by depth as well as by ordered speed. From the graphs, it is evident that slow speeds provide the highest likelihood of entanglement. Further, the shallow depth tested resulted in significant reduction in the likelihood of entanglement.

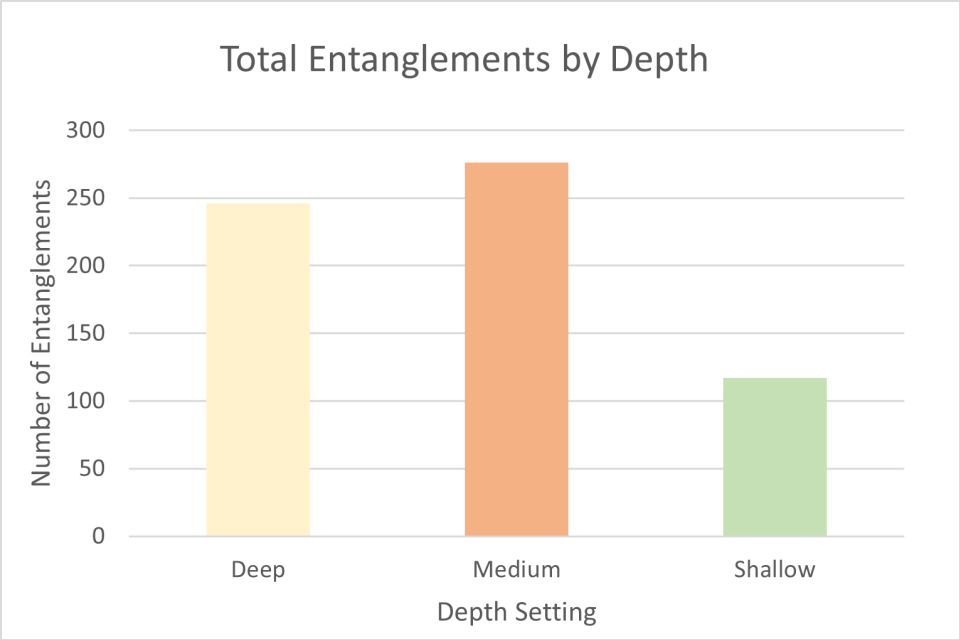

(a) Total # of Entanglements by Depth

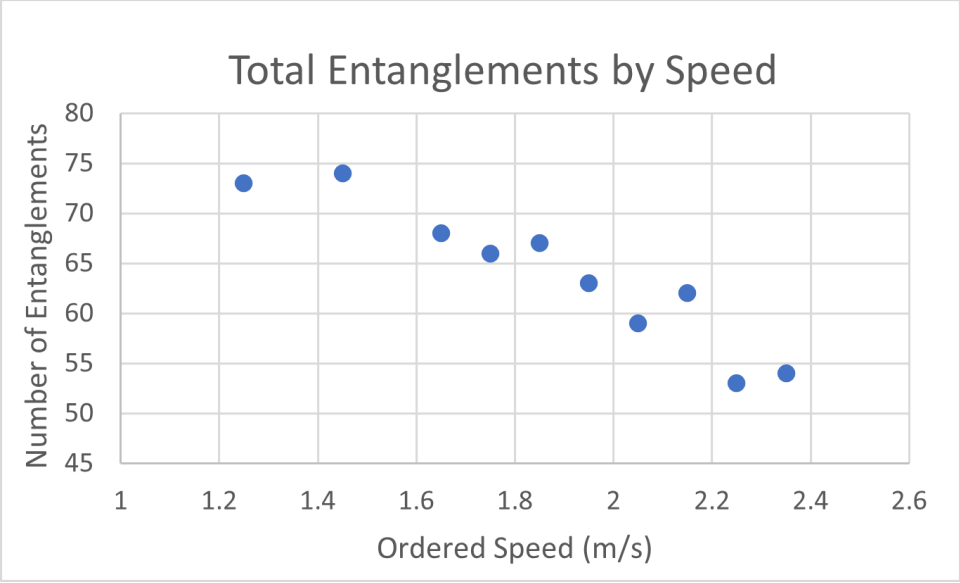

(b) Total # of Entanglements by Speed

Figure 4.2. Total Entanglements Per Varied Conditions (Depth and Speed)

4.2.2 Weighted Scale

The results in the following sections provide color scale representations for the data collected at each depth. Since each set of data is based on the 10 runs performed at each condition, the scale shown in Figure 4.3 applies to both the entanglement and the level of influence results. The number corresponds to the sum of the weights applied for each experienced result as defined in the taxonomy.

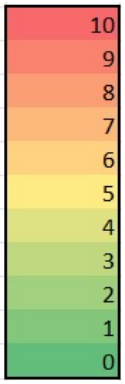

Figure 4.3. Color Scale with Number Corresponding to Weighted Taxonomy

4.2.3 Shallow Depth

Unlike the results seen in the medium depth tests, the levels of influence plot did not mirror the entanglement results closely. While those regions that showed high levels of entanglement also showed a great deal of interaction, the amount of influence caused on the eelgrass was much greater across the range of lateral separation. These results, shown below, suggest a correlation between the outcomes of the study and the depth in relation to the free length of the eelgrass.

Entanglement Likelihood at Shallow Depth

When the vehicle was placed at shallow depth, the outcome changed dramatically from the tests run at the medium depth setting. The likelihood of entanglement dropped substantially as shown in Figure 4.4. Entanglement was only consistent with the vehicle placed centerline. Still, shallow depths provided the greatest number of occlusion events of any trial. The only entanglement that occurred with the propeller on the right was at the slowest speed settings.

With the propeller on the right, the likelihood of entanglement increased but remained much lower when compared to the medium depth trials. At shallow depth, it is evident that the risk of entanglement is lower both at high speeds and when the propeller is on the right side of the eelgrass.

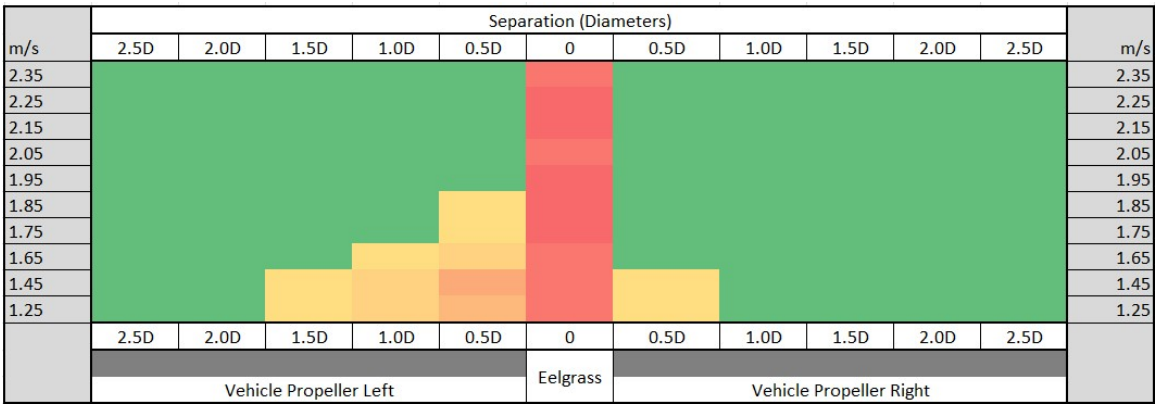

Figure 4.4. Shallow Depth Entanglement Likelihood

Levels of Influence at Shallow Depth

In contrast to the entanglement likelihood at shallow depth, the interaction between the propeller and the eelgrass increased significantly during these tests. Figure 4.5 shows propeller influence on the eelgrass occurred over a much wider range of separation distances when compared to the medium depth tests. Conventional wisdom may cause you to see a higher level of interaction and assume a greater likelihood of entanglement; however, in this trial that was not the case. The propeller caused significant disruption of the eelgrass out to 1.5-2.0 diameters but no corresponding entanglements. Still, this test depth saw a much higher percentage of occlusion events than any other trial. This may be attributed to the available free length of eelgrass relative to its anchor. Manipulation of the free end of the eelgrass appears to occur much more freely, while the reduced length above the propeller may make it more difficult for the eelgrass to wrap on itself. While the eelgrass moves easily with the slightest disturbance, there is less material that can be pulled over and around the propeller and its hub. This appears to result in the increasing level of influence observed while decreasing the likelihood of entanglement.

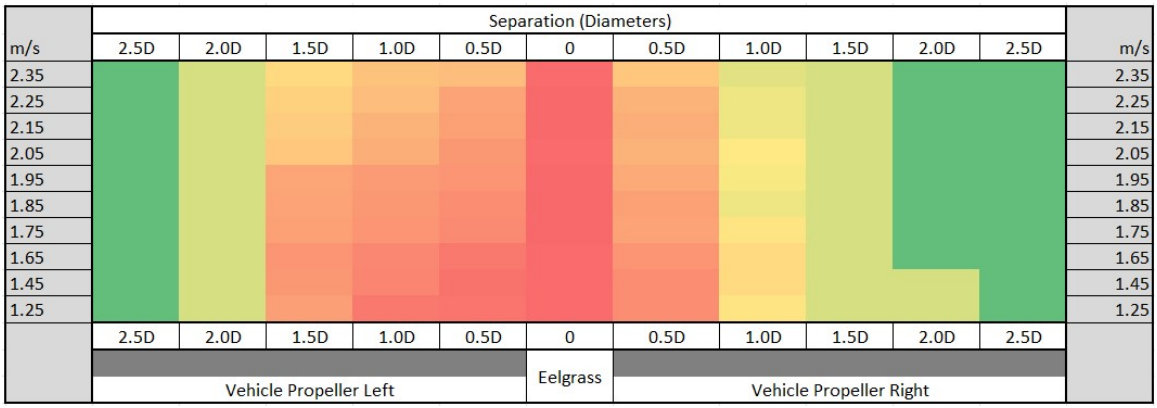

Figure 4.5. Levels of Influence at Shallow Depth

4.2.4 Medium Depth

Entanglement Likelihood at Medium Depth

The first experiments conducted in the full DOE for unrestricted vehicle movement occurred at medium depth (50.80 cm from eelgrass base). This height provided a depth near the middle of the eelgrass and offers the most practical simulation of expected submerged UUV operations within eelgrass beds. The data in Appendix B Table B.1 represents each test in the DOE conducted at this depth. Figure 4.6 shows only the likelihood of entanglement based on a given condition at this depth. The data represents trials conducted out to 2.5 times the diameter of the propeller in lateral separation. However, in this trial, events further away than 1.5 times the diameter recorded zero entanglement events. Runs conducted at this depth with no lateral separation showed entanglement events nearly every trial. Though this figure shows only entanglement events, it is important to note that when the vehicle was placed centerline, as well as half of a diameter to the left of the eelgrass, each event that did not result in entanglement resulted in occlusion events.

The test results shown in Figure 4.6 indicate an asymmetry beginning at the 0.5D lateral separation. The entanglement occurrences, specifically at higher speeds, were significantly fewer on the right side than when the eelgrass was passed on the left side at the same separation. At lower speeds, the likelihood of entanglement was significant at one diameter with the propeller on the left, and nearly non-existent when the propeller passed on the right side. Furthermore, an interesting discovery occurred at one diameter for the propeller on the

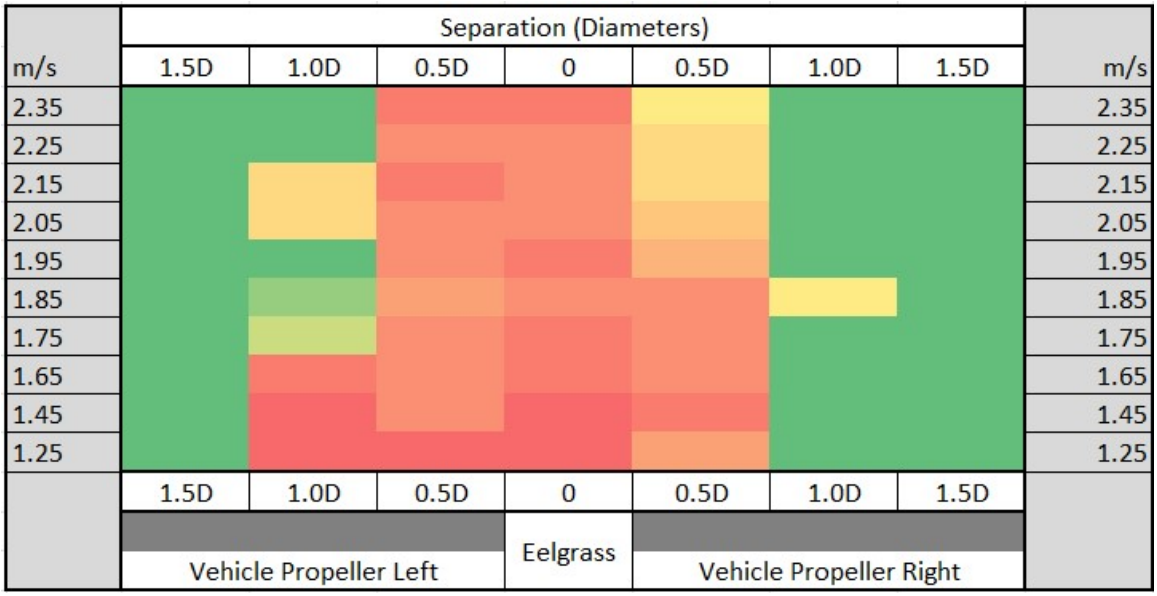

Figure 4.6. Medium Depth Entanglement Likelihood

left side. Based on other trials at high-speed, the likelihood may be expected to significantly decrease as speed increases. However, after decreasing substantially once the speed reached 1.75, the likelihood of entanglement increases at speeds of 2.05 m/s and 2.15 m/s. The likelihood then drops to zero and remains there as speed is further increased. One possible explanation for this occurrence is a change in the flow pattern or flow regime, similar to fluid transitioning from laminar to turbulent flow, around the propeller at this RPM range. That possibility is not explored in this study, but may be relevant for future work.

Levels of Influence at Medium Depth

Figure 4.7's representation of the varying levels of influence caused on the eelgrass by the vehicle's propeller closely resembles the entanglement likelihood modeled in Figure 4.6. However, it shows a much larger area of influence than the entanglement results reveal. The figure also affirms an asymmetric nature to the interactions between the eelgrass and propeller at this depth.

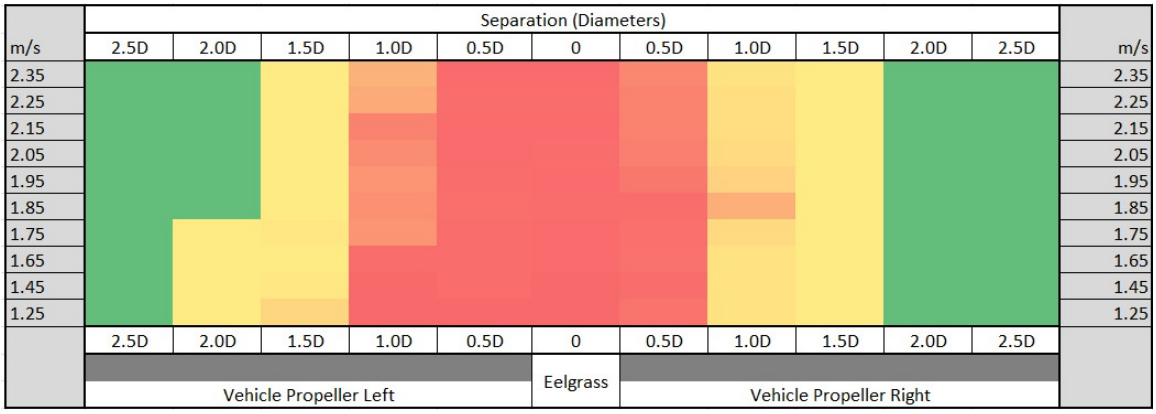

Figure 4.7. Levels of Influence at Medium Depth

4.2.5 Deep Depth

Once again, depth as a variable appears to be a significant factor in this study. The trials at deep depth show interesting developments in relation to the speed and likelihood of entanglement. Much like the previous trials, the entanglement events nearly all occur where there exists no lateral separation between the tip of the propeller and the eelgrass. However, previous trials produced an increased likelihood for entanglement at slower speeds. The tests conducted at deep depth produced a different result.

Entanglement Likelihood at Deep Depth

At deep depth, the propeller appeared to require both a minimum speed and a minimum amount of time alongside the eelgrass to cause entanglement. With the vehicle at centerline, the results were not dissimilar to those conducted at other depths. When the vehicle was moved to the left at 0.5D, the likelihood of entanglement was high at all speeds. This was not the case for the vehicle placed on the right side. At this condition, the propeller did not entangle until the vehicle reached 1.75 m/s ordered speed. Outside of 0.5D on this side, the vehicle never entangled. With the vehicle moved to one diameter on the left side, the likelihood of entanglement was reduced at low speeds, increased when speeds were between 1.65-2.15 m/s, and subsided entirely at higher speeds. These results suggest two competing factors at play that affect entanglement: the time spent alongside the eelgrass and the amount of force generated by the propeller to pull the eelgrass down into the propeller. The vehicle's ordered speed correlates to the RPM of the propeller. This RPM generates a certain amount

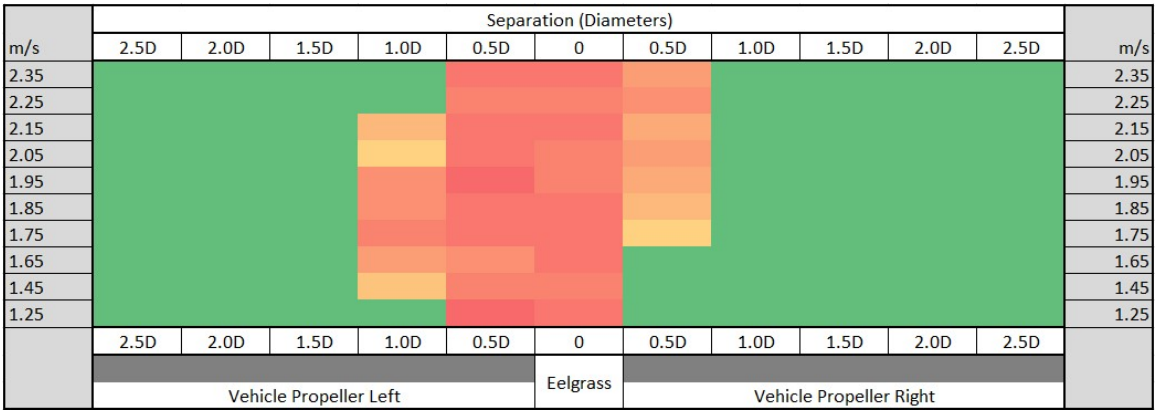

Figure 4.8. Deep Depth Entanglement Likelihood

of thrust that relates to the speed and momentum of the fluid being moved past the propeller. This movement of the fluid presumably pulls the eelgrass into the propeller. At deeper depths, there appears to be a minimum force required to pull the length of the eelgrass down and over the propeller. The results in Figure 4.8 suggest that this minimum force begins to occur at an ordered speed of 1.45m/s. There is also a minimum amount of time required for the eelgrass to be pulled down and wrap around the propeller and its hub. As the speed increases, the time that the propeller spends alongside the eelgrass decreases. Therefore, there appears to be a maximum tested speed of 2.15 m/s that produces the force required to pull the eelgrass in, but reduces the amount of time spent alongside to such a degree as to nearly eliminate the risk of entanglement.

Levels of Influence at Deep Depth

The amount of influence in this trial, shown in Figure 4.9, resembles the results of the entanglement events at this depth. However, the minimum and maximum speeds discussed in relation to entanglement events do not necessarily provide as clear conclusions when looking at the level of influence. While some delineation exists in the figure, the speeds which showed no entanglement risk show moderate levels of influence. The scope of the interactions are much broader, stretching out to 1.5D-2.0D, but this amount of influence does not necessarily result in entanglement events. This supports the conclusion that there is a minimum amount of force required to pull the eelgrass into entanglement. The moderate to high levels of influence above 2.15 m/s at one diameter on the left side also supports the

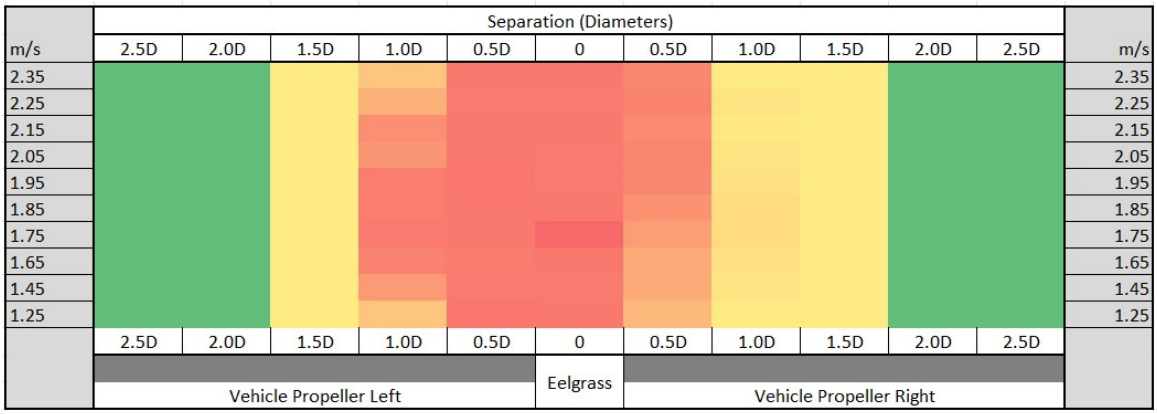

Figure 4.9. Levels of Influence at Deep Depth

assertion that there is a minimum amount of time needed for the eelgrass to be pulled down and around the propeller since these runs did not result in entanglement events.

4.3 Analysis of Asymmetry

In review of the results presented in this chapter, a significant asymmetry exists in the likelihood of entanglement of a single propeller with marine vegetation such as eelgrass. This asymmetry is exacerbated by certain test conditions. At deeper depths, variation in speed results in clearer asymmetry than changes in lateral separation. While speed, specifically lower speed, is still important at shallow depths, the scope of entanglement risk expands to wider lateral separations. At medium depths, where the most entanglement events occurred, fewer occlusions occurred and speeds followed a pattern of entanglement reduction as ordered velocity increased. With the vehicle passing on the right side of the eelgrass, little risk of entanglement exists at any tested depth outside of 0.5 diameters. On the opposite side, however, entanglement risk exists at all depths out to at least one diameter. Based on the results presented in Table 4.2, only 27.5% of entanglements that did not occur with the vehicle at centerline did so with the vehicle on the right side of the eelgrass. This analysis of asymmetry, due to the direction of propeller rotation, provides an opportunity to inform operating procedures and vehicle design for UUVs in the littorals that could reduce the likelihood of entanglement.

THIS PAGE INTENTIONALLY LEFT BLANK

CHAPTER 5:
Conclusions and Future Work

The results and analysis presented in Chapter 4 showed a clear asymmetry in the likelihood of entanglement depending on which side of the propeller the vegetation was on. Furthermore, the results indicate a correlation between the different variables tested, such as depth, speed, and lateral separation, that can reduce or increase the likelihood of entanglement on each side. The results and analysis in Chapter 4 were reviewed and used to make key conclusions about this study and provide a basis for future work to more definitively define some of the resulting relationships.

5.1 Conclusions

This study showed that the likelihood of entanglement for a propeller given a single strand of eelgrass is not dependent on a single factor. Additionally, while multiple factors affect the likelihood, their effects are not independent. Instead, these variables showed a dependency on each other that suggests the impacts of these variables change as conditions change. Depth, for instance, shows remarkable correlation to the amount of speed required to cause entanglement. Furthermore, lateral separation appears to be correlated to the side of passage as well as the speed of the vehicle. Regardless of the other factors, the vehicle's passage on the propeller's downward rotation side of the eelgrass reduced the number of entanglement events. This fact proves that asymmetry is integral in the determination of the likelihood of entanglement.

5.1.1 Lateral Separation and Time Alongside Eelgrass

As expected, the vehicle's proximity to the eelgrass was a significant factor in the likelihood of entanglement. At shallow depths, the amount of influence felt on the eelgrass by the propeller at further separations was greater, but this resulted in few entanglements. While the amount of influence indicates a significant interaction, this suggests that there may not have been enough eelgrass to wrap around itself and cause entanglement. This conclusion is also supported by the results at the deep depth testing. While greater speeds were needed

to see an increase in entanglement events, once the vehicle reached a certain speed, it would pass the eelgrass too quickly and entanglement events dropped to zero.

Given an interaction with a shroud-less propeller and marine vegetation, such as eelgrass, these results show that a small lateral separation combined with slow speeds provides significantly increased likelihood of entanglement. If a UUV must operate at medium or shallow depths, higher speeds should be utilized and passage on the propeller downward rotation side of the eelgrass is preferred. This test was conducted with the vehicle operating in reverse with a UUV that has fixed propeller pitch. As such, operating in this direction simply reverses the direction of rotation of the propeller. Therefore, if a vehicle were operating in the forward direction, the propeller would spin clockwise and passage on the left side of the eelgrass would be preferred. At deeper depths, time alongside the eelgrass is not as concerning until moderate speeds are reached. Therefore, the vehicle should operate with at least 0.5 diameters of separation and operate at either very low or very high speeds.

5.1.2 Asymmetry

This study set out to determine if an asymmetric relationship exists for the likelihood of entanglement with marine vegetation for a single propeller UUV. By analyzing the interactions of the propeller with a single strand and removing additional factors that affect entanglement, such as fins, shrouds, or vehicle shape [3], each set of tests revealed that significant asymmetry exists based on the direction of a propeller's rotation. On the side that the propeller made contact with the eelgrass, if the direction of rotation of the propeller was upward, the risk of entanglement was significantly higher than when it was moving downward.

If a UUV must operate in a marine vegetation field, the understanding of this asymmetry can be key. Ultimately, given a choice, a UUV should operate with the direction of rotation pointed down at contact as described above. However, likelihood of entanglement in those conditions still varies and can change operating procedures. If the UUV is operating in shallow water, a higher speed should provide fewer occasions of entanglement. At medium depth, this also holds true, but the moderate speeds tested also provide higher chance of entanglement that they did not at shallow depths. If operating in deep water, the slowest speeds which proved most costly at medium depth can actually substantially reduce the

likelihood of entanglement. These same conclusions are not mirrored when the side of operation changes as the scope of entanglement likelihood widens significantly.

5.2 Future Work

5.2.1 Future Work Related to This trial

Future work to continue this trial could prove useful in many different avenues. While even intervals of lateral separation and mostly standard step sizes of 0.1 m/s for speed provided sufficient data to draw conclusions on asymmetry, more fidelity in both of those areas could lead to the identification of the actual location of boundaries that demarcate significant changes in the likelihood of entanglement. Further extrapolating the depths at which the vehicle was operated could also provide an understanding of the impact the amount of free or tethered eelgrass has on the likelihood of entanglement.

With respect to further exploring the role of the eelgrass in the experiment, future work could explore the specific manner in which the eelgrass becomes wrapped. It could explore any relationship with the apparent randomness of occlusion events and the factors that may affect it. Lastly, more work could be done to define whether the force required to pull the eelgrass into entanglement changes based on the distance from the eelgrass's anchor or the amount of free end.

5.2.2 Flow Pattern Relationship with RPM and Entanglement

While the future work presented above relates directly to results from this trial, more work could be done to bridge the gap between work done on the efficiency of propellers and the resulting flow pattern and the flow pattern's relationship to entanglement. This trial saw a few unexpected results based on vehicle's speed changes. There were regions noted in Chapter 4 where certain speed ranges increased the likelihood of entanglement before it dropped off at higher speeds. Additionally, slow speeds at deep depths showed a tendency to avoid entanglement. A possible explanation for these anomalies is the changing nature of the propeller's flow pattern as the velocity increases or decreases. If there is a non-linear relationship between RPM and the radius of the flow pattern, future work might explore the resulting effects on the likelihood of entanglement.

THIS PAGE INTENTIONALLY LEFT BLANK

APPENDIX A:
DREW UV Operating Manual

This appendix serves as an operating manual for the DREW UV. This vehicle is still in development at NSWC Panama City. For questions concerning operation, troubleshooting, or applicable files, contact NSWC Panama City.

A.1 Vehicle Procedures (VP)

Step VP-1. Remove vehicle, battery container, Microhard PDDL2450 and power adapter, and Polyken 827 roll from Pelican Case.

Step VP-2. Remove tail section from UUV by pulling and rotating white 3D printed tail cone.

***Note:** *Take care not to remove further then battery carriage from vehicle. Doing so can unplug various data cables.*

Step VP-3. Remove battery from packaging and connect to power connector in DREW UV as shown in Figure A.1

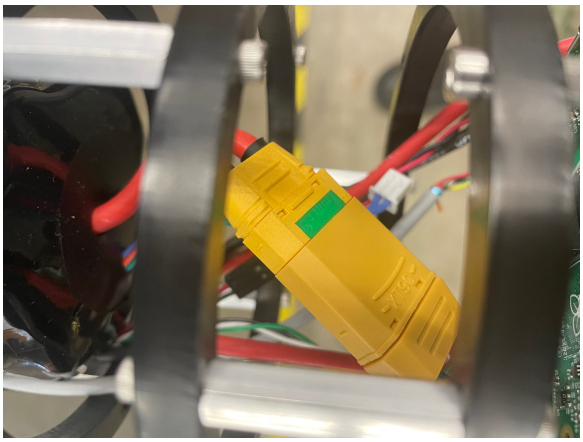

Figure A.1. Battery Connected to DREW UV

Step VP-4. Place battery on rails and secure around stanchions with velcro straps as shown in Figure A.2

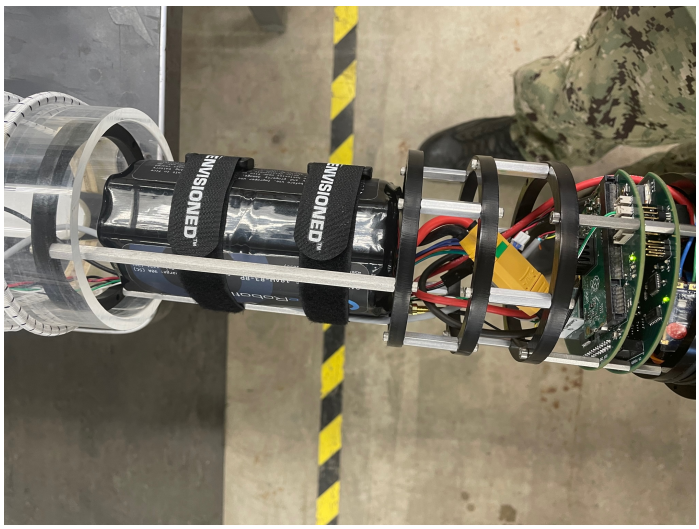

Figure A.2. DREW UV Tail Piece Removed and Battery Inserted

Step VP-5. Ensure uFL mast data coaxial cable is firmly secured to the "main" terminal on the Microhard modem inside the vehicle as shown in Figure A.3

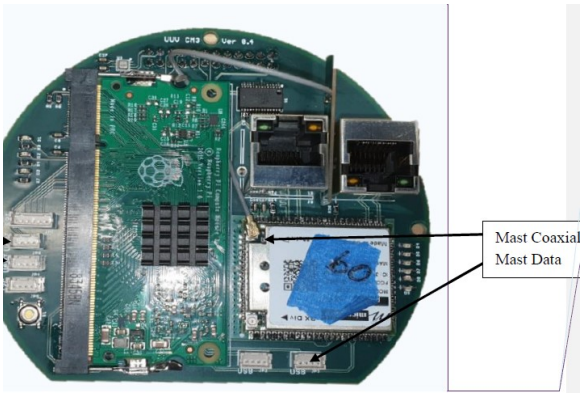

Figure A.3. Mast Data uFL Cable connected to Microhard Modem on Vehicle Aft Computer Board

Step VP-6. Re-insert the tail piece of the vehicle into the main body

***Note:** The vehicle will take approximately 60 seconds to fully boot. The vehicle will beep when the battery is initially plugged in, and then again once the onboard PC has fully started*

***Note:** After vehicle boot, verify that the light indicated in Figure A.4 is flashing*

Figure A.4. DREW UV Mast Showing Indicator Light

Step VP-7. Wrap the seam where the main body meets the nose cone with Polyken 827 waterproofing tape a minimum of 1.5 times. Repeat this step for the aft seam shown in Figure A.5

Figure A.5. Aft Section of DREW UV Shown Wrapped with Polyken Tape at Aft Seam

Step VP-8. Insert Vent Plug marked “OK”, shown in Figure A.6, in the nose cone and ensure tight

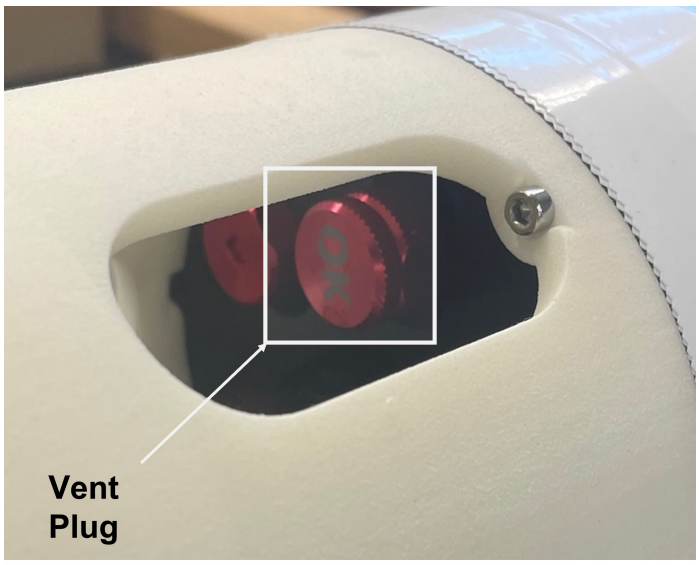

Figure A.6. Vent Plug Inserted in Nose Cone

A.2 Network Setup (NS)

This vehicle requires the use of a graphical user interface provided by NSWC PC. These files can be obtained from Dr. Joseph Klamo at the Naval Postgraduate School in Monterey, CA or from NSWC Panama City.

Step NS-1. Download the zip file for either Windows or Linux

***Note:** This thesis utilized Windows. The steps do not change for use with Linux, but contact NSWC PC for support.*

Step NS-2. Open the computer’s network adapter settings.

Step NS-3. Select the computer’s ethernet port and view additional properties

Step NS-4. Change the IP assignment to “Static” or “Manual” and assign an IP address on the 192.168.168 subnet. The static IP address should be 192.168.168.xx(x).

**Note:* *This thesis used IP address 192.168.168.107*

Step NS-5. Connect the ethernet port on the computer to the Microhard PDDL2450's LAN Port

Step NS-6. Connect the antenna to the Microhard's Antenna 1 receptacle and plug in power adapter

**Note:* *The Microhard will automatically connect to the modem on the vehicle. But, the GUI most be launched in order to control the vehicle.*

Step NS-7. Open the command prompt on the computer

Step NS-8. Navigate to the directory that contains web_server_only.js file within the command prompt

Step NS-9. Execute the command: node web_serve_only.js 3000

Step NS-10. Open a browser and in the address bar navigate to localhost:3000

**Note:* *This should load the GUI shown in Figure A.7*

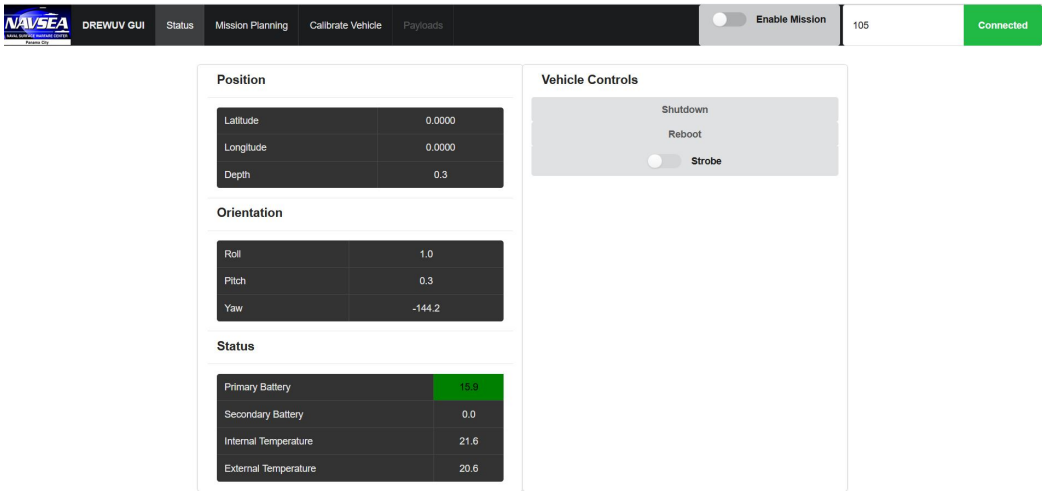

Figure A.7. DREW UV GUI Showing Connection

Step NS-11. In the upper right hand corner, enter the vehicle's hull number and hit connect

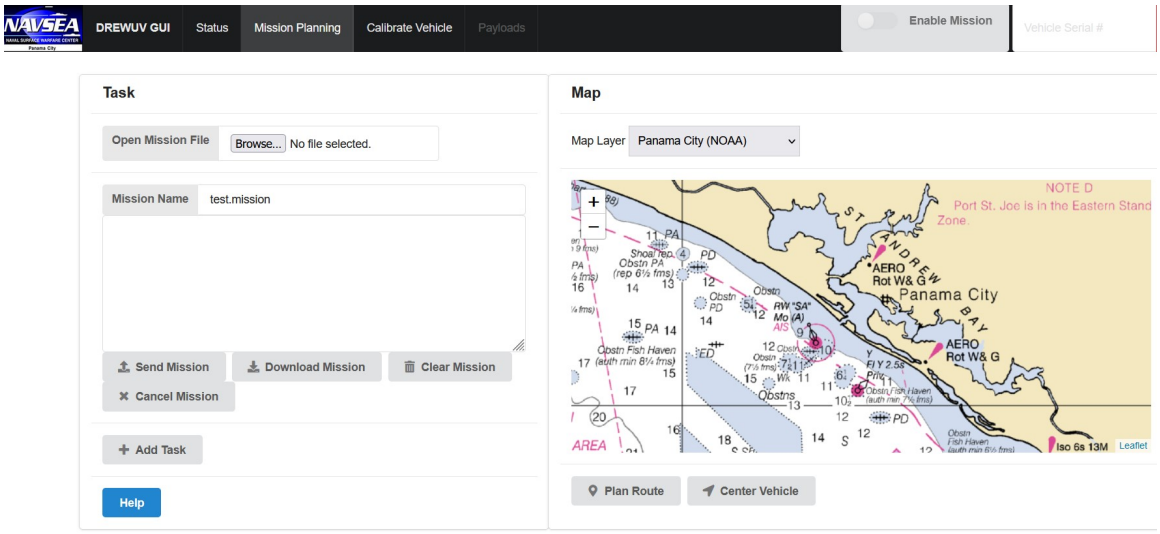

Figure A.8. Mission Planning Page Used to Build and Upload Mission Package to DREW UV

***Note:** This should change the "Connect" button to green and produce vehicle statistics in the status page shown in Figure A.7*

***Note:** If the Microhard's wireless signal bars are cycling, unplug the Microhard and reset the DREW UV utilizing the included magnet and technical manual*

A.3 Mission Planning (MP)

Step MP-1. From the Menu selection bar at the top of the page, select the "Mission Planning" Tab. This will load the page shown in Figure A.8

***Note:** For first time mission package build, follow steps MP-2 through MP-5. If loading a previously built package, select "Browse..." next to "Open Mission File." Navigate to saved filed on PC and select "OK." Then proceed to Step MP-6*

Step MP-2. Select the "+ Add Task" button highlighted in Figure A.9

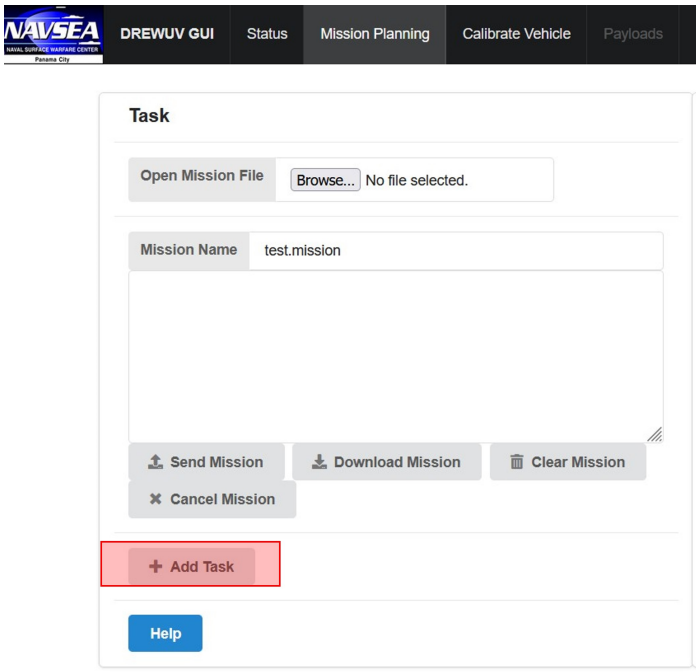

Figure A.9. Add Task Button Selected During Build Mission Process

Step MP-3. Select task option from the drop-down highlighted in Figure A.10

Figure A.10. Add Task Menu Used to Add Setpoint and Wait Commands to Build Mission Packages

***Note.** This experiment only utilized the "Wait" and "Setpoint" task options. Numerous other tasks are available including waypoint, loiter, dive, and fix that were not needed for*

this study. In the "Setpoint" task option, only speed and duration were specified since the heading and depth were fixed

Step MP-3a. If selecting "Wait", specify the duration in seconds and click "+ Add Task"

Step MP-3b. If selecting "Setpoint", specify the speed in m/s and the duration in seconds. Click "+ Add Task"

Step MP-4. Repeat steps MP-2 and MP-3 until the full package is built

Step MP-5. Next to "Mission Name" specify the package name and click "Download Mission" to save the mission package for future use

***Note:** Ensure one return line exists after last added task or this package will not load for future use*

Step MP-6. Ensure vehicle is in position to accept mission package

Step MP-7. Click the "Send Mission" button highlighted in Figure A.11. Ensure the button turns green

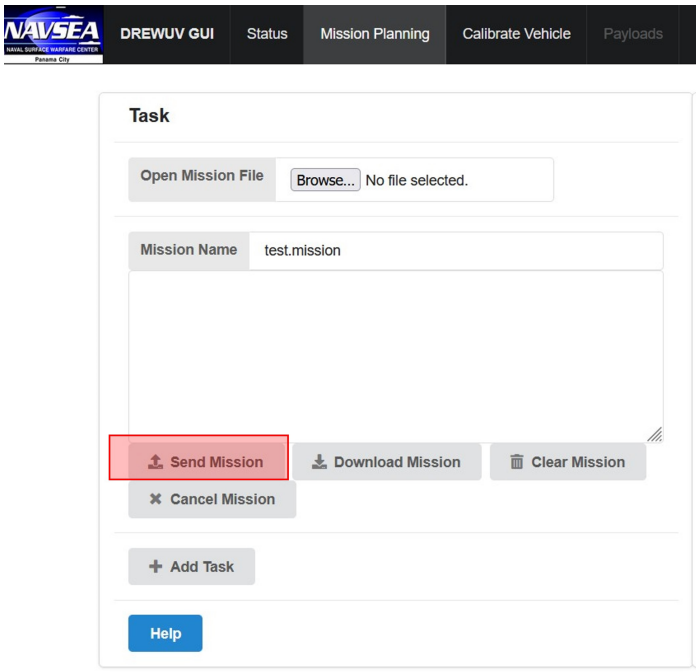

Figure A.11. Highlighted Send Mission Selected for Mission Upload

Step MP-8. Click the "Enable Mission" toggle switch in the upper right hand corner as highlighted in Figure A.12

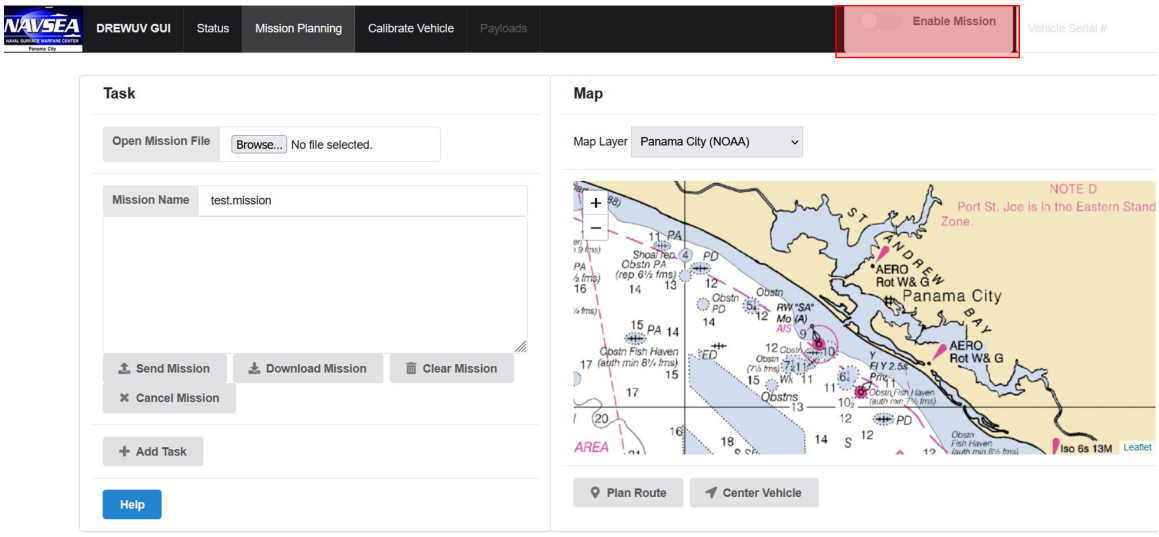

Figure A.12. Enable Mission Toggle Switch Used to Transmit to Vehicle and Execute

***Note:** Toggle switch may only remain switched on while transmitting package. After package upload, toggle switch will appear off*

APPENDIX B:
DOE Data

Table B.1. Design of Experiments Test Matrix

Four Factor Full Factorial DOE											
Shallow Depth Testing											
Speed	Left Passage						Right Passage				
(m/s)	2.5D	2.0D	1.5D	1.0D	0.5D	0.0	0.5D	1.0D	1.5D	2.0D	2.5D
1.25	N	L	H	O	O	E	O	M	L	L	N
1.25	N	L	H	O	O	E	H	M	L	L	N
1.25	N	L	M	O	E	E	O	L	L	L	N
1.25	N	L	H	O	E	O	H	L	L	L	N
1.25	N	L	H	O	E	E	E	M	L	L	N
1.25	N	L	M	O	O	E	H	L	L	L	N
1.25	N	L	H	E	O	E	H	M	L	L	N
1.25	N	L	H	O	O	E	O	L	L	L	N
1.25	N	L	E	O	E	E	H	M	L	L	N
1.25	N	L	H	E	O	E	H	L	L	L	N
1.45	N	L	H	O	O	E	H	M	L	L	N
1.45	N	L	E	E	E	E	O	L	L	L	N
1.45	N	L	H	H	E	E	H	M	L	L	N
1.45	N	L	H	E	E	E	H	M	L	L	N
1.45	N	L	M	O	O	E	H	M	L	L	N
1.45	N	L	H	O	O	E	H	L	L	L	N
1.45	N	L	H	H	E	E	E	M	L	L	N
1.45	N	L	H	H	O	O	O	L	L	L	N
1.45	N	L	O	O	E	E	H	M	L	L	N
1.45	N	L	H	H	O	E	O	M	L	L	N
1.65	N	L	H	O	E	E	O	M	L	N	N

1.65	N	L	O	H	O	E	H	M	L	N	N
1.65	N	L	H	H	O	E	H	L	L	N	N
1.65	N	L	H	H	O	E	O	M	L	N	N
1.65	N	L	H	O	O	E	H	L	L	N	N
1.65	N	L	H	E	O	E	H	L	L	N	N
1.65	N	L	O	O	O	E	H	M	L	N	N
1.65	N	L	H	O	E	E	H	M	L	N	N
1.65	N	L	H	H	O	E	H	M	L	N	N
1.65	N	L	H	O	O	O	H	M	L	N	N
1.75	N	L	H	O	O	E	H	L	L	N	N
1.75	N	L	H	H	E	E	H	M	L	N	N
1.75	N	L	O	H	H	E	M	L	L	N	N
1.75	N	L	H	H	O	E	O	L	L	N	N
1.75	N	L	H	H	O	E	M	L	L	N	N
1.75	N	L	M	H	H	E	H	M	L	N	N
1.75	N	L	H	H	H	E	H	M	L	N	N
1.75	N	L	H	O	O	E	O	L	L	N	N
1.75	N	L	H	H	H	E	M	M	L	N	N
1.75	N	L	M	H	H	E	H	M	L	N	N
1.85	N	L	H	O	O	E	H	L	L	N	N
1.85	N	L	M	H	H	E	H	L	L	N	N
1.85	N	L	H	H	H	E	H	L	L	N	N
1.85	N	L	M	H	H	E	H	M	L	N	N
1.85	N	L	H	H	H	E	H	L	L	N	N
1.85	N	L	H	H	O	E	M	M	L	N	N
1.85	N	L	H	H	H	E	H	L	L	N	N
1.85	N	L	H	H	O	E	M	L	L	N	N
1.85	N	L	H	H	E	E	H	L	L	N	N
1.85	N	L	H	H	H	E	O	L	L	N	N
1.95	N	L	H	H	H	E	H	L	L	N	N
1.95	N	L	H	H	H	E	M	L	L	N	N
1.95	N	L	H	H	H	E	O	L	L	N	N

1.95	N	L	M	H	H	E	H	L	L	N	N
1.95	N	L	H	H	O	E	M	M	L	N	N
1.95	N	L	H	H	H	E	M	M	L	N	N
1.95	N	L	M	H	O	E	H	L	L	N	N
1.95	N	L	H	H	H	E	H	M	L	N	N
1.95	N	L	M	H	H	E	M	L	L	N	N
1.95	N	L	O	H	H	E	H	L	L	N	N
2.05	N	L	M	H	H	E	H	L	L	N	N
2.05	N	L	M	H	H	E	H	M	L	N	N
2.05	N	L	H	H	H	E	H	L	L	N	N
2.05	N	L	M	M	H	O	M	L	L	N	N
2.05	N	L	M	H	H	E	M	L	L	N	N
2.05	N	L	M	H	H	E	H	L	L	N	N
2.05	N	L	M	M	H	E	H	M	L	N	N
2.05	N	L	M	M	O	E	M	L	L	N	N
2.05	N	L	M	H	H	E	H	M	L	N	N
2.05	N	L	M	M	H	E	H	M	L	N	N
2.15	N	L	M	H	H	E	M	L	L	N	N
2.15	N	L	M	H	H	E	H	L	L	N	N
2.15	N	L	M	M	M	E	H	L	L	N	N
2.15	N	L	M	H	O	E	H	L	L	N	N
2.15	N	L	M	H	H	E	M	M	L	N	N
2.15	N	L	L	M	H	E	M	M	L	N	N
2.15	N	L	M	M	M	E	M	L	L	N	N
2.15	N	L	M	M	H	E	H	L	L	N	N
2.15	N	L	M	M	H	E	H	L	L	N	N
2.15	N	L	H	H	H	E	H	L	L	N	N
2.25	N	L	M	M	H	E	M	L	L	N	N
2.25	N	L	M	M	H	E	H	L	L	N	N
2.25	N	L	M	H	H	E	H	L	L	N	N
2.25	N	L	L	M	H	E	H	L	L	N	N
2.25	N	L	M	M	M	E	M	L	L	N	N

2.25	N	L	M	M	H	E	H	M	L	N	N
2.25	N	L	H	M	H	E	M	L	L	N	N
2.25	N	L	M	H	H	E	M	L	L	N	N
2.25	N	L	L	H	H	E	H	L	L	N	N
2.25	N	L	M	M	M	E	M	M	L	N	N
2.35	N	L	M	M	M	E	M	L	L	N	N
2.35	N	L	M	M	H	E	M	M	L	N	N
2.35	N	L	M	H	H	E	M	L	L	N	N
2.35	N	L	M	H	M	E	M	L	L	N	N
2.35	N	L	L	M	H	E	M	L	L	N	N
2.35	N	L	L	M	H	O	H	L	L	N	N
2.35	N	L	M	M	H	E	M	L	L	N	N
2.35	N	L	M	M	M	E	M	L	L	N	N
2.35	N	L	L	M	M	E	M	L	L	N	N
2.35	N	L	M	M	H	E	M	L	L	N	N

Medium Depth Testing											
Speed	Left Passage						Right Passage				
(m/s)	2.5D	2.0D	1.5D	1.0D	0.5D	0.0	0.5D	1.0D	1.5D	2.0D	2.5D
1.25	N	L	L	E	E	E	E	L	L	N	N
1.25	N	L	M	E	E	E	H	L	L	N	N
1.25	N	L	M	E	E	E	E	L	L	N	N
1.25	N	L	L	E	E	E	E	L	L	N	N
1.25	N	L	L	E	E	E	O	L	L	N	N
1.25	N	L	M	E	E	E	H	L	L	N	N
1.25	N	L	L	E	E	E	E	M	L	N	N
1.25	N	L	L	E	E	E	E	M	L	N	N
1.25	N	L	L	E	E	E	E	L	L	N	N
1.25	N	L	H	E	E	E	E	L	L	N	N
1.45	N	L	L	E	O	E	E	L	L	N	N
1.45	N	L	L	E	E	E	E	L	L	N	N
1.45	N	L	L	E	E	E	H	L	L	N	N
1.45	N	L	L	E	E	E	E	L	L	N	N

1.45	N	L	L	E	E	E	E	M	L	N	N
1.45	N	L	L	E	O	E	E	L	L	N	N
1.45	N	L	L	E	E	E	E	L	L	N	N
1.45	N	L	L	E	E	E	E	M	L	N	N
1.45	N	L	M	E	E	E	E	L	L	N	N
1.45	N	L	L	E	E	E	E	L	L	N	N
1.65	N	L	L	H	E	E	E	L	L	N	N
1.65	N	L	L	E	O	E	E	L	L	N	N
1.65	N	L	L	E	E	E	E	L	L	N	N
1.65	N	L	L	E	O	E	E	L	L	N	N
1.65	N	L	L	E	E	E	E	L	L	N	N
1.65	N	L	L	E	E	O	H	M	L	N	N
1.65	N	L	L	E	E	E	E	L	L	N	N
1.65	N	L	L	E	E	E	H	L	L	N	N
1.65	N	L	L	E	E	E	E	M	L	N	N
1.65	N	L	L	E	E	E	E	L	L	N	N
1.75	N	L	L	L	E	E	E	L	L	N	N
1.75	N	L	L	H	E	E	E	M	L	N	N
1.75	N	L	M	H	E	E	E	M	L	N	N
1.75	N	L	L	E	E	E	H	M	L	N	N
1.75	N	L	L	H	O	E	E	L	L	N	N
1.75	N	L	L	H	E	E	E	L	L	N	N
1.75	N	L	L	H	O	E	E	M	L	N	N
1.75	N	L	L	H	E	E	E	L	L	N	N
1.75	N	L	L	H	E	O	O	L	L	N	N
1.75	N	L	L	E	E	E	E	L	L	N	N
1.85	N	N	L	H	E	E	E	L	L	N	N
1.85	N	N	L	H	E	E	E	L	L	N	N
1.85	N	N	L	E	E	E	E	M	L	N	N
1.85	N	N	L	H	O	E	E	M	L	N	N
1.85	N	N	L	H	E	E	O	E	L	N	N
1.85	N	N	L	H	E	E	O	E	L	N	N

1.85	N	N	L	H	O	O	E	M	L	N	N
1.85	N	N	L	H	E	E	E	M	L	N	N
1.85	N	N	L	H	E	O	E	E	L	N	N
1.85	N	N	L	H	O	E	E	M	L	N	N
1.95	N	N	L	H	E	E	O	M	L	N	N
1.95	N	N	L	H	E	E	E	M	L	N	N
1.95	N	N	L	H	E	E	E	L	L	N	N
1.95	N	N	L	H	E	E	E	M	L	N	N
1.95	N	N	L	H	E	E	H	M	L	N	N
1.95	N	N	L	H	O	E	E	L	L	N	N
1.95	N	N	L	H	O	E	H	M	L	N	N
1.95	N	N	L	H	E	E	E	L	L	N	N
1.95	N	N	L	H	E	O	E	M	L	N	N
1.95	N	N	L	H	E	E	H	L	L	N	N
2.05	N	N	L	H	O	E	H	L	L	N	N
2.05	N	N	L	H	E	E	E	M	L	N	N
2.05	N	N	L	E	E	O	E	L	L	N	N
2.05	N	N	L	E	E	E	H	M	L	N	N
2.05	N	N	L	H	E	E	E	L	L	N	N
2.05	N	N	L	H	E	E	E	L	L	N	N
2.05	N	N	L	H	E	E	E	L	L	N	N
2.05	N	N	L	H	E	E	H	M	L	N	N
2.05	N	N	L	H	E	E	H	M	L	N	N
2.05	N	N	L	H	E	O	H	L	L	N	N
2.15	N	N	L	H	E	E	H	L	L	N	N
2.15	N	N	L	E	E	O	E	L	L	N	N
2.15	N	N	L	E	E	E	H	M	L	N	N
2.15	N	N	L	H	E	E	H	L	L	N	N
2.15	N	N	L	E	E	E	H	L	L	N	N
2.15	N	N	L	H	E	E	E	M	L	N	N
2.15	N	N	L	H	E	E	H	L	L	N	N
2.15	N	N	L	H	E	E	E	L	L	N	N

2.15	N	N	L	H	E	E	E	L	L	N	N
2.15	N	N	L	E	O	E	H	M	L	N	N
2.25	N	N	L	H	O	O	E	L	L	N	N
2.25	N	N	L	H	O	E	E	L	L	N	N
2.25	N	N	L	H	E	E	H	L	L	N	N
2.25	N	N	L	M	E	E	H	L	L	N	N
2.25	N	N	L	M	E	E	H	M	L	N	N
2.25	N	N	L	H	E	E	H	M	L	N	N
2.25	N	N	L	M	E	E	H	L	L	N	N
2.25	N	N	L	M	E	O	E	L	L	N	N
2.25	N	N	L	M	E	E	E	M	L	N	N
2.25	N	N	L	H	E	E	H	L	L	N	N
2.35	N	N	L	H	E	E	H	L	L	N	N
2.35	N	N	L	M	E	O	H	L	L	N	N
2.35	N	N	L	M	E	E	E	L	L	N	N
2.35	N	N	L	H	E	E	E	M	L	N	N
2.35	N	N	L	M	E	E	H	L	L	N	N
2.35	N	N	L	M	O	E	H	L	L	N	N
2.35	N	N	L	M	E	E	H	L	L	N	N
2.35	N	N	L	M	E	E	E	M	L	N	N
2.35	N	N	L	M	E	E	H	L	L	N	N
2.35	N	N	L	H	E	E	H	L	L	N	N

Deep Depth Testing											
Speed	Left Passage						Right Passage				
(m/s)	2.5D	2D	1.5D	D	0.5D	0	0.5D	D	1.5D	2D	2.5D
1.25	N	N	L	L	E	E	M	L	L	N	N
1.25	N	N	L	M	E	O	M	L	L	N	N
1.25	N	N	L	M	E	E	H	L	L	N	N
1.25	N	N	L	H	E	E	M	L	L	N	N
1.25	N	N	L	M	E	E	L	L	L	N	N
1.25	N	N	L	H	E	E	M	L	L	N	N
1.25	N	N	L	L	E	E	H	L	L	N	N

1.25	N	N	L	M	E	E	H	L	L	N	N
1.25	N	N	L	M	E	E	M	L	L	N	N
1.25	N	N	L	M	E	E	H	L	L	N	N
1.45	N	N	L	M	O	E	H	L	L	N	N
1.45	N	N	L	H	E	E	H	L	L	N	N
1.45	N	N	L	H	E	E	M	L	L	N	N
1.45	N	N	L	M	E	E	H	L	L	N	N
1.45	N	N	L	H	E	E	H	L	L	N	N
1.45	N	N	L	H	O	O	M	M	L	N	N
1.45	N	N	L	E	E	O	H	M	L	N	N
1.45	N	N	L	H	E	E	M	L	L	N	N
1.45	N	N	L	E	E	E	H	L	L	N	N
1.45	N	N	L	E	E	E	H	L	L	N	N
1.65	N	N	L	E	E	E	M	M	L	N	N
1.65	N	N	L	O	O	E	H	L	L	N	N
1.65	N	N	L	E	E	E	M	L	L	N	N
1.65	N	N	L	H	O	E	H	L	L	N	N
1.65	N	N	L	O	E	E	H	M	L	N	N
1.65	N	N	L	E	E	O	H	L	L	N	N
1.65	N	N	L	E	E	E	H	M	L	N	N
1.65	N	N	L	H	O	E	H	L	L	N	N
1.65	N	N	L	E	E	E	M	L	L	N	N
1.65	N	N	L	E	E	E	H	L	L	N	N
1.75	N	N	L	E	E	E	H	M	L	N	N
1.75	N	N	L	E	E	E	M	L	L	N	N
1.75	N	N	L	E	E	E	E	M	L	N	N
1.75	N	N	L	O	E	E	H	M	L	N	N
1.75	N	N	L	E	E	E	M	L	L	N	N
1.75	N	N	L	O	E	E	H	L	L	N	N
1.75	N	N	L	E	E	E	E	L	L	N	N
1.75	N	N	L	E	E	O	H	M	L	N	N
1.75	N	N	L	E	O	E	H	L	L	N	N

1.75	N	N	L	E	E	E	H	L	L	N	N
1.85	N	N	L	O	E	E	H	L	L	N	N
1.85	N	N	L	E	E	E	H	L	L	N	N
1.85	N	N	L	E	E	E	E	L	L	N	N
1.85	N	N	L	O	E	O	H	M	L	N	N
1.85	N	N	L	E	E	E	H	L	L	N	N
1.85	N	N	L	E	E	E	H	M	L	N	N
1.85	N	N	L	E	E	E	H	M	L	N	N
1.85	N	N	L	E	O	E	H	L	L	N	N
1.85	N	N	L	E	E	E	E	M	L	N	N
1.85	N	N	L	H	E	E	E	L	L	N	N
1.95	N	N	L	E	E	E	E	L	L	N	N
1.95	N	N	L	E	E	E	H	L	L	N	N
1.95	N	N	L	E	E	E	H	M	L	N	N
1.95	N	N	L	O	E	E	H	L	L	N	N
1.95	N	N	L	E	E	E	E	L	L	N	N
1.95	N	N	L	O	E	E	E	M	L	N	N
1.95	N	N	L	E	E	O	H	M	L	N	N
1.95	N	N	L	E	E	O	E	L	L	N	N
1.95	N	N	L	H	E	E	E	L	L	N	N
1.95	N	N	L	E	E	E	E	L	L	N	N
2.05	N	N	L	H	O	E	E	L	L	N	N
2.05	N	N	L	H	E	E	H	M	L	N	N
2.05	N	N	L	E	E	O	O	L	L	N	N
2.05	N	N	L	E	E	E	E	L	L	N	N
2.05	N	N	L	H	E	E	H	L	L	N	N
2.05	N	N	L	H	E	E	H	M	L	N	N
2.05	N	N	L	H	E	E	E	L	L	N	N
2.05	N	N	L	H	E	E	E	L	L	N	N
2.05	N	N	L	H	E	E	E	L	L	N	N
2.05	N	N	L	H	E	O	E	L	L	N	N
2.15	N	N	L	H	E	E	E	L	L	N	N

2.15	N	N	L	E	E	O	E	L	L	N	N
2.15	N	N	L	E	E	E	H	L	L	N	N
2.15	N	N	L	H	E	E	E	L	L	N	N
2.15	N	N	L	E	E	E	H	L	L	N	N
2.15	N	N	L	H	E	E	E	L	L	N	N
2.15	N	N	L	H	E	E	H	M	L	N	N
2.15	N	N	L	H	E	E	H	L	L	N	N
2.15	N	N	L	H	E	E	H	L	L	N	N
2.15	N	N	L	E	O	E	E	L	L	N	N
2.25	N	N	L	H	O	O	E	M	L	N	N
2.25	N	N	L	H	O	E	E	L	L	N	N
2.25	N	N	L	H	E	E	E	M	L	N	N
2.25	N	N	L	M	E	E	E	L	L	N	N
2.25	N	N	L	M	E	E	H	L	L	N	N
2.25	N	N	L	H	E	E	H	L	L	N	N
2.25	N	N	L	M	E	E	E	L	L	N	N
2.25	N	N	L	M	E	O	E	L	L	N	N
2.25	N	N	L	M	E	E	H	L	L	N	N
2.25	N	N	L	H	E	E	E	L	L	N	N
2.35	N	N	L	H	E	E	E	L	L	N	N
2.35	N	N	L	M	E	O	H	L	L	N	N
2.35	N	N	L	M	E	E	E	L	L	N	N
2.35	N	N	L	H	E	E	E	L	L	N	N
2.35	N	N	L	M	E	E	E	L	L	N	N
2.35	N	N	L	M	O	E	E	L	L	N	N
2.35	N	N	L	M	E	E	H	L	L	N	N
2.35	N	N	L	M	E	E	H	L	L	N	N
2.35	N	N	L	M	E	E	H	L	L	N	N
2.35	N	N	L	H	E	E	E	L	L	N	N

List of References

[1] T. Simmons, MCC, USN, "Effective mine countermeasure training at exercise northern coasts 2019," Accessed May 28, 2022 [Online]. Available: https://www.c6f.navy.mil/Press-Room/News/News-Display/Article/1960934/effective-mine-countermeasure-training-at-exercise-northern-coasts-2019/

[2] Department of the Navy, "The Navy unmanned underwater vehicle (UUV) master plan," Department of the Navy, Washington, DC, USA, Washington, DC: USA, 2004 [Online]. Available: https://www.hsdl.org/?view&did=708654

[3] K. Irgens, "Experimental assessment of entanglement for unmanned underwater vehicle with an open three-bladed propeller," M.S. thesis, Dept. of Eng. and Appl. Sci., NPS, Monterey, CA, USA, 2020 [Online]. Available: http://hdl.handle.net/10945/66660

[4] G. Anuat, "Investigating interactions between a box-shaped unmanned underwater vehicle and marine vegetation," M.S. thesis, Dept. of Eng. and Appl. Sci., NPS, Monterey, CA, USA, 2021 [Online]. Available: http://hdl.handle.net/10945/68693

[5] D. of Defense, "Autonomous undersea vehicle requirement for 2025," Washington, DC: USA, 2016 [Online]. Available: https://news.usni.org/wp-content/uploads/2016/03/18Feb16-Report-to-Congress-Autonomous-Undersea-Vehicle-Requirement-for-2025.pdf

[6] Northeast Ocean Data, "Updated regional eelgrass map," Accessed May 28, 2022 [Online]. Available: https://www.northeastoceandata.org/updated-regional-eelgrass-map/

[7] Cornell University Cooperative Extension of Suffolk County, "Taxonomy of eelgrass zostera marina," Accessed May 15, 2022 [Online]. Available: http://www.seagrassli.org/ecology/eelgrass/taxonomy.html

[8] National Oceanic and Atmospheric Administration Fisheries, "The importance of eelgrass," Accessed Apr 4, 2022 [Online]. Available: https://www.fisheries.noaa.gov/feature-story/importance-eelgrass

[9] R. Murphy, L. Orzetti, and W. Johnson, *Plant fact sheet for eelgrass(Zostera marina)*, USDA, Natural Resources Conservation Service, Norman A. Berg National Plant Materials Center. Beltsville, MD 2012 [Online]. Available: https://www.nrcs.usda.gov/Internet/FSE_PLANTMATERIALS/publications/mdpmcfs10921.pdf

[10] P. Shively, "Six reasons to protect eelgrass," PEW, June 7, 2019 [Online]. Available: https://www.pewtrusts.org/en/research-and-analysis/articles/2019/06/07/six-reasons-to-protect-eelgrass

[11] Blue Robotics, "T200 thruster," Accessed May 28, 2022 [Online]. Available: https://bluerobotics.com/store/thrusters/t100-t200-thrusters/t200-thruster-r2-rp/

[12] B. Xin, L. Xiaohui, S. Zhaocun, and Z. Yuquan, "A vectored water jet propulsion method for autonomous underwater vehicles," *Ocean Engineering*, vol. 74, p. 133–140, 2013.

[13] Naval News Staff, "Hii's remus 300 selected as U.S. Navy's next gen small UUV," Accessed May 30, 2022 [Online]. Available: https://www.navalnews.com/naval-news/2022/03/hiis-remus-300-selected-as-u-s-navys-next-gen-small-uuv/

[14] A. Suzuki, H. Kondo, and M. Osakabe, "Water jet Propulsion Mechanism for Low Speed AUV," in *Proceedings of the International Symposium on Marine Engineering (ISME) October 15-19, 2017, Tokyo, Japan*, 2017 [Online]. Available: https://www2.kaiyodai.ac.jp/~osakabe/ISMEAUV.pdf

[15] R. Duelley, "Autonomous underwater vehicle propulsion design," M.S. thesis, Virginia Polytechnic Institute and State University, Blacksburg, VA, USA, 2010 [Online]. Available: https://vtechworks.lib.vt.edu/bitstream/handle/10919/34789/Duelley_RS_T_2010.pdf?sequence=1

[16] J. Wu, Y. Dou, H. Lv, C. Ma, L. Zhong, S. Xu, and X. Han, "Thrust Characteristics of a Ducted Propeller and Hydrodynamics of an Underwater Vehicle in Control Motions," in *Journal of Marine Science and Engineering*, 2021 [Online]. Available: https://doi.org/10.3390/jmse9090940

[17] K. Irgens, J. Klamo, and A. Pollman, "Experimental assessment of entanglement for a propeller-driven unmanned underwater vehicle," *Naval Engineers Journal*, vol. 133, no. 23, Sep. 2021.

[18] G. Anuat, J. Klamo, and A. Pollman, "Effects of body geometry and propulsion type on unmanned underwater vehicle interactions with marine vegetation," *ASME Journal of Autonomous Vehicles and Systems*, vol. under review, 2021.

[19] *Disposable Reusable Expeditionary Warfare Unmanned Underwater Vehicle (DREW UV) Systems Procedures*, TM MSPQ-030 Rev N, NAVSEA, Naval Surface Warfare Center, Panama City, FL, USA, 2019.

Initial Distribution List

1. Defense Technical Information Center
   Ft. Belvoir, Virginia

2. Dudley Knox Library
   Naval Postgraduate School
   Monterey, California